tion profiles of the cardiovascular system. They should also provide a basis for further characterization of the importance of epigenetic alterations in the development of cardiac hypertrophy or heart failure. Application of DCS to human heart specimens has the potential to highlight such information of clinical relevance.

Acknowledgments

This work was supported in part by a Grant-in-Aid for Scientific Research on Priority Areas (C) "Medical Genome Science" from the Ministry of Education, Culture, Sports, Science, and Technology of Japan and by a grant from Salt Science Research Foundation (#04C7).

References

1. Baylin SB, Herman JG. DNA hypermethylation in tumorigenesis: epigenetics joins genetics. *Trends Genet.* 2000;16:168–174.
2. van Leeuwen F, Gottschling DE. Genome-wide histone modifications: gaining specificity by preventing promiscuity. *Curr Opin Cell Biol.* 2002; 14:756–762.
3. Burgess-Beusse B, Farrell C, Gaszner M, Litt M, Mutskov V, Recillas-Targa F, Simpson M, West A, Felsenfeld G The insulation of genes from external enhancers and silencing chromatin. *Proc Natl Acad Sci U S A.* 2002;99:16433–16437.
4. Carrozza MJ, Utley RT, Workman JL, Cote J. The diverse functions of histone acetyltransferase complexes. *Trends Genet.* 2003;19:321–329.
5. Verdin E, Dequiedt F, Kasler HG. Class II histone deacetylases: versatile regulators. *Trends Genet.* 2003;19:286–293.
6. Gusterson RJ, Jazrawi E, Adcock IM, Latchman DS. The transcriptional co-activators CREB-binding protein (CBP) and p300 play a critical role in cardiac hypertrophy that is dependent on their histone acetyltransferase activity. *J Biol Chem.* 2003;278:6838–6847.
7. Iezzi S, Di Padova M, Serra C, Caretti G, Simone C, Maklan E, Minetti G, Zhao P, Hoffman EP, Puri PL, Sartorelli V. Deacetylase inhibitors increase muscle cell size by promoting myoblast recruitment and fusion through induction of follistatin. *Dev Cell.* 2004;6:673–684.
8. Zhang CL, McKinsey TA, Chang S, Antos CL, Hill JA, Olson EN. Class II histone deacetylases act as signal-responsive repressors of cardiac hypertrophy. *Cell.* 2002;110:479–488.
9. Kook H, Lepore JJ, Gitler AD, Lu MM, Wing-Man Yung W, Mackay J, Zhou R, Ferrari V, Gruber P, Epstein JA. Cardiac hypertrophy and histone deacetylase-dependent transcriptional repression mediated by the atypical homeodomain protein Hop. *J Clin Invest.* 2003;112:863–871.
10. Antos CL, McKinsey TA, Dreitz M, Hollingsworth LM, Zhang CL, Schreiber K, Rindt H, Gorczynski RJ, Olson EN. Dose-dependent blockade to cardiomyocyte hypertrophy by histone deacetylase inhibitors. *J Biol Chem.* 2003;278:28930–28937.
11. Kuwahara K, Saito Y, Ogawa E, Takahashi N, Nakagawa Y, Naruse Y, Harada M, Hamanaka I, Izumi T, Miyamoto Y, Kishimoto I, Kawakami R, Nakanishi M, Mori N, Nakao K. The neuron-restrictive silencer element-neuron-restrictive silencer factor system regulates basal and endothelin 1-inducible atrial natriuretic peptide gene expression in ventricular myocytes. *Mol Cell Biol.* 2001;21:2085–2097.
12. Kaneda R, Toyota M, Yamashita Y, Koinuma K, Choi YL, Ota J, Kisanuki H, Ishikawa M, Takada S, Shimada K, Mano H. High-throughput screening of genome fragments bound to differentially acetylated histones. *Genes Cells.* 2004;9:1167–1174.
13. Yamamoto K, Dang QN, Kelly RA, Lee RT. Mechanical strain suppresses inducible nitric-oxide synthase in cardiac myocytes. *J Biol Chem.* 1998;273:11862–11866.
14. Kent WJ. BLAT–the BLAST-like alignment tool. *Genome Res.* 2002;12: 656–664.
15. Rat Genome Sequencing Project Consortium. Genome sequence of the Brown Norway rat yields insights into mammalian evolution. *Nature.* 2004;428:493–521.
16. Marks AR. Cardiac intracellular calcium release channels: role in heart failure. *Circ Res.* 2000;87:8–11.
17. Kapinya KJ, Harms U, Harms C, Blei K, Katchanov J, Dirnagl U, Hortnagl H. Role of NAD(P)H:quinone oxidoreductase in the progression of neuronal cell death in vitro and following cerebral ischaemia in vivo. *J Neurochem.* 2003;84:1028–1039.
18. Shawber C, Nofziger D, Hsieh JJ, Lindsell C, Bogler O, Hayward D, Weinmaster G. Notch signaling inhibits muscle cell differentiation through a CBF1-independent pathway. *Development.* 1996;122: 3765–3773.
19. Henderson C, Brancolini C. Apoptotic pathways activated by histone deacetylase inhibitors: implications for the drug-resistant phenotype. *Drug Resist Updat.* 2003;6:247–256.
20. Chen QM, Tu VC, Wu Y, Bahl JJ. Hydrogen peroxide dose dependent induction of cell death or hypertrophy in cardiomyocytes. *Arch Biochem Biophys.* 2000;373:242–248.
21. Onan D, Pipolo L, Yang E, Hannan RD, Thomas WG. Urotensin II promotes hypertrophy of cardiac myocytes via mitogen-activated protein kinases. *Mol Endocrinol.* 2004;18:2344–2354.
22. Fingert JH, Heon E, Liebmann JM, Yamamoto T, Craig JE, Rait J, Kawase K, Hoh ST, Buys YM, Dickinson J, Hockey RR, Williams-Lyn D, Trope G, Kitazawa Y, Ritch R, Mackey DA, Alward WL, Sheffield VC, Stone EM. Analysis of myocilin mutations in 1703 glaucoma patients from five different populations. *Hum Mol Genet.* 1999;8: 899–905.
23. Bernstein BE, Kamal M, Lindblad-Toh K, Bekiranov S, Bailey DK, Huebert DJ, McMahon S, Karlsson EK, Kulbokas EJ 3rd, Gingeras TR, Schreiber SL, Lander ES. Genomic maps and comparative analysis of histone modifications in human and mouse. *Cell.* 2005;120:169–181.
24. Weinmann AS, Yan PS, Oberley MJ, Huang TH, Farnham PJ. Isolating human transcription factor targets by coupling chromatin immunoprecipitation and CpG island microarray analysis. *Genes Dev.* 2002;16:235–244.
25. Turner BM, O'Neill LP. Histone acetylation in chromatin and chromosomes. *Semin Cell Biol.* 1995;6:229–236.
26. Strahl BD, Allis CD. The language of covalent histone modifications. *Nature.* 2000;403:41–45.

ELSEVIER

European Journal of Cancer 41 (2005) 2170–2175

European Journal of Cancer

www.ejconline.com

Retroviral expression screening of oncogenes in pancreatic ductal carcinoma

Hiroyuki Kisanuki [a], Young Lim Choi [a], Tomoaki Wada [a], Ryozo Moriuchi [b], Shin-ichiro Fujiwara [a], Ruri Kaneda [a], Koji Koinuma [a], Madoka Ishikawa [a], Shuji Takada [a], Yoshihiro Yamashita [a], Hiroyuki Mano [a,c,*]

[a] *Division of Functional Genomics, Jichi Medical School, 3311-1 Yakushiji, Kawachigun, Tochigi 329-0498, Japan*
[b] *Department of Molecular Microbiology and Immunology, Nagasaki University Graduate School of Medicine, Nagasaki, Japan*
[c] *CREST, Japan Science and Technology Agency, Saitama, Japan*

Received 4 March 2005; received in revised form 3 May 2005; accepted 10 May 2005
Available online 25 August 2005

Abstract

Pancreatic ductal carcinoma (PDC) remains one of the most intractable malignancies in humans. In order to clarify the molecular events underlying the carcinogenesis in PDC, we constructed a retroviral cDNA expression library from a PDC cell line, and used it to screen transforming genes in PDC by a focus formation assay with mouse 3T3 fibroblasts. We could obtain a total of 30 transformed cell foci in the screening, and one of the cDNA inserts harvested from such cell clones turned out to encode a wild-type human ARAF1. Unexpectedly, a long terminal repeat-driven overexpression of *ARAF1* mRNA was confirmed to induce transformed foci in fibroblasts. The oncogenic potential of ARAF1 was examined by injecting the transformed fibroblasts into athymic nude mice. Importantly, *ARAF1* mRNA was highly expressed in pancreatic ductal cell specimens purified from patients with PDC. These results have unveiled the transforming potential of ARAF1 protein, and also suggest that quantity of intracellular ARAF1 may be important in carcinogenesis of various human cancers.

Keywords: Pancreatic ductal cell carcinoma; Retrovirus; ARAF1; cDNA library; Oncogene

1. Introduction

Pancreatic ductal carcinoma (PDC) originates from pancreatic ductal cells, and is one of the most intractable malignancies in humans [1,2]. Effective therapy for PDC is hampered by the lack of specific clinical symptoms. At the time of diagnosis, most patients are no longer candidates for surgical resection, and, even in individuals who do undergo such surgery, the 5-year survival rate is only 20–30% [1].

Vast efforts have been made to elucidate molecular events responsible for the carcinogenesis of PDC. Mutations of *TP53* gene can be, for instance, found in PDC specimens [3], and in the intraductal *in situ* regions as well [4]. Similarly, inactivation has been found for other tumour-suppressor genes, such as DPC, RB1 and p16 [5].

As for oncogenes, activating mutations in the *KRAS2* gene has been reported to be frequently associated with PDC [6]. The same *KRAS2* mutations could be, however, found in the samples for chronic pancreatitis [7], making their pathogenetic role uncertain. Additionally, an increased telomerase activity was shown to be present only in PDC, but not in nonmalignant pancreatic disorders [8]. Again, however, others could detect an elevated telomerase activity in chronic pancreatitis and normal

* Corresponding author. Tel.: +81 285 58 7449; fax: +81 285 44 7322.
E-mail address: hmano@jichi.ac.jp (H. Mano).

0959-8049/$ - see front matter © 2005 Elsevier Ltd. All rights reserved.
doi:10.1016/j.ejca.2005.05.014

pancreas [9]. Therefore, it is yet to be revealed which transforming genes truly promote a clonal growth of pancreatic ductal cells.

For an efficient isolation of tumour-promoting genes in PDC, it would be desirable to conduct functional screening based on transforming ability. Focus formation assays with mouse 3T3 fibroblasts have been highly successful for the identification of oncogenes in human cancer [10]. In such screening, genomic DNA is isolated from cancer specimens, and used to transfect 3T3 cells to obtain transformed cell foci. It should be noted, however, that, since expression of any genes in these experiments are driven by their own promoters/enhancers, oncogenes in PDC can exert their effects in 3T3 cells only when the promoter/enhancer regions of such genes are active in fibroblasts, which is not always guaranteed.

To ensure the sufficient expression of cDNAs in 3T3 cells, their transcription should be regulated by an exogenous promoter fragment. We have therefore constructed a retroviral cDNA expression library from a PDC cell line, MiaPaCa-2, which was used to infect 3T3 cells. In the preparation of cDNA library, we further took advantage of the SMART polymerase chain reaction (PCR) system (Clontech, Palo Alto, CA), which preferentially amplifies full-length cDNAs. A focus formation assay with the library resulted in an identification of a transforming *ARAF1* gene.

2. Materials and methods

2.1. Cells and culture

MiaPaCa-2, Capan-2, PANC-1, 3T3, and BOSC23 [11] cell lines were obtained from American Type Culture Collection, and maintained in Dulbecco's modified Eagle medium/F12 (DMEM/F12; Invitrogen, Carlsbad, CA) containing 10% fetal bovine serum (Invitrogen) and 2 mM L-glutamine.

The fresh clinical specimens were obtained from patients who gave informed consent, and the study was approved by the institutional review board of Jichi Medical School. Cells were collected from the pancreatic juice by centrifugation, labeled with anti-MUC1 antibody [12] (Novocastra Laboratories, Newcastle upon Tyne, UK), and subjected to chromatography on a miniMACS magnetic cell separation column (Miltenyi Biotec, Auburn, CA) [13]. The purity of the resultant $MUC1^+$ cell fraction was confirmed by staining with Wright Giemmsa solutions and microscopy examination for each case (data not shown).

2.2. Retrovirus library construction

Total RNA was extracted from MiaPaCa-2 cells by an RNeasy Mini column with RNase-free DNase (Qiagen, Valencia, CA), and the first strand cDNA was synthesized by PowerScript reverse transcriptase (Clontech) with SMART IIA oligonucleotide and CDS primer IIA (both from Clontech). The cDNAs were then amplified for 12 cycles with 5′ PCR primer IIA according to the instruction of the SMART PCR cDNA synthesis kit (Clontech) except a substitution of LA Taq polymerase (Takara Bio, Shiga, Japan) for Advantage 2 DNA polymerase provided with the kit. Resultant cDNAs were treated with proteinase K, blunt-ended by T4 DNA polymerase, and ligated to the BstXI-adaptor (Invitrogen). Unbound adaptors were removed through the cDNA size fractionation column (Invitrogen), and the cDNAs were finally ligated to the pMXS retroviral plasmid (a kind gift of Dr. T. Kitamura at Institute of Medical Science, University of Tokyo) [14] digested with BstXI. The pMXS-cDNA plasmids were introduced into ElecroMax DH10B cells (Invitrogen) with electroporation.

2.3. Focus formation assay

Generation of recombinant retroviral library and focus formation assay was conducted as described previously [15]. Briefly, BOSC23 cells were transfected with Lipfectamin reagent (Invitrogen) and 2 μg of retroviral plasmid together with 0.5 μg of pGP plasmid 0.5 μg of pE-eco plasmid (both from Takara Bio). Two days after the transfection, polybrene (Sigma, St. Louis, MI) was added to the culture supernatant at a concentration of 4 μg/ml, and the supernatant was subsequently used to infect 3T3 cells for 48 h. For the focus formation assay, the culture medium of 3T3 cells was then changed to DMEM-high glucose (Invitrogen) supplemented with 5% calf serum and 2 mM L-glutamine. Transformed foci were picked up after 3 weeks of culture. Genomic DNA was extracted from each transformed focus, and was subjected to PCR with 5′ PCR primer IIA (Clontech) and LA Taq polymerase for 50 cycles of 98 °C for 20 s and 68 °C for 6 min. Amplified genome fragments were purified for nucleotide sequencing. For tumorgenicity assay in nude mice, transformed 3T3 cells were injected into each shoulder of nu/nu Balb-c mice (6 weeks old). Tumour formation was assessed after 4 weeks.

2.4. "Real-time" RT-PCR

Portions of oligo(dT)-primed cDNA were subjected to PCR with a QuantiTect SYBR Green PCR Kit (Qiagen). The amplification protocol was comprised of incubations at 94 °C for 15 s, 57 °C for 30 s, and 72 °C for 60 s. Incorporation of the SYBR Green dye into PCR products was monitored in real time with an ABI PRISM 7900HT sequence detection system (PE Applied Biosystems, Foster City, CA), thereby allowing determination of the threshold cycle (C_T) at which exponential amplification of products

begins. The C_T values for cDNAs corresponding to the β-actin gene (*ACTB*) and to the *ARAF1* gene were used to calculate the abundance of the latter mRNA relative to that of the former. The oligonucleotide primers for PCR were as follows: 5′-CCATCATGAAGTGTGACGTGG-3′ and 5′-GTCCGCCTAGAAGCATTTGCG-3′ for *ACTB*, and 5′-ACTACCTCCATGCCAAGAACATCA-3′ and 5′-GACGTCTGACTGGAAGCTGTAGGG-3′ for *ARAF1*.

3. Results

3.1. Screening with focus formation assay

From mRNA of MiaPaCa-2 cells, full-length cDNAs were selectively amplified and ligated to a retroviral vector pMXS. We could obtain a total of 2.1×10^6 colony forming units (cfu) of independent plasmid clones. Thirty clones were randomly selected from the library, and examined for the incorporated cDNAs. Twenty-seven (90%) out of the 30 clones contained inserts with an average length of 2.05 kbp.

By introducing the plasmid DNA into a packaging cell line, we generated a recombinant ecotropic retrovirus library that was subsequently used to infect mouse 3T3 fibroblasts. Infection experiments were repeated for a total of 6 times. After 3 weeks of culture, 30 transformed foci were observed (Fig. 1(b)). No foci could be found among the cells infected with an empty virus (Fig. 1(a)), while numerous foci were easily identified in the cells infected with a virus expressing v-Ras oncoprotein (Fig. 1(c)).

Each focus was isolated, expanded independently, and was subject to the extraction of genomic DNA. We then tried to recover retroviral inserts from the genomic DNA by PCR amplification with the primer used originally to amplify the cDNAs in the construction of the library. In most cases, two to three DNA fragments were recovered from each genome (Fig. 2(a)), implying a multiple retroviral infection on the recipient 3T3 cells.

We obtained a total of 56 cDNA fragments by PCR, all of which were subjected to nucleotide sequencing from both ends. Screening of the cDNA sequences against human genome sequence database assembled as of July 2003 by the Genome Bioinformatics Group of the University of California at Santa Cruz (http://genome.ucsc.edu) revealed that the 56 fragments correspond to 13 independent genes, eleven of which could be matched at >95% identity to the human genome sequence (Table 1). Among the 11 genes, 7 of them were known genes while the rest 4 were unknown. Each cDNA clone was ligated to pMXS in both directions, and a recombinant retrovirus was generated from each resultant plasmid. Transforming ability of the cDNAs was thus confirmed by a focus formation assay with the recombinant virus.

Focus formation assays were conducted for the 26 independent viruses (all 13 independent genes for both directions), and one of them, expressing ARAF1 protein (GenBank accession number, NM_001654), gave transformed foci in repeated experiments. ARAF1 belongs to

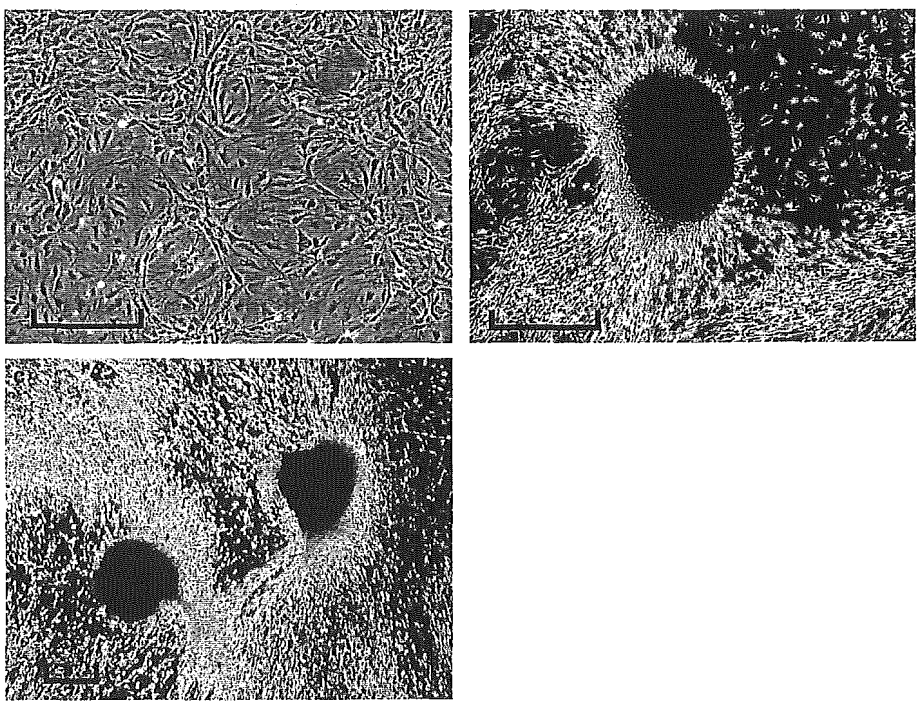

Fig. 1. Focus formation assay with retroviral library. Mouse 3T3 cells were infected with (a) an empty virus, (b) retroviruses from the MiaPaCa-2 library, or (c) a retrovirus expressing v-Ras as a positive control. Pictures were taken after 3 weeks of culture. Scale bar, 100 μm.

Table 1
cDNAs isolated from 3T3 transformants

Clone #	Gene symbol	GenBank number	Covering full ORF
1	Unknown	AK026325	ND
2	No homologues sequences	ND	ND
3	Unknown	AF318370	Yes
4	PITPNM1	NM_004910	No
5	Unknown	BC022099	Yes
6	DECR2	NM_020664	Yes
7	ARAF1	NM_001654	Yes
8	BCLG	NM_138724	No
9	No homologues sequences	ND	ND
10	Unknown	AL607122	ND
11	JAG1	NM_000214	Yes
12	MRPL43	NM_176792	Yes
13	PLOD3	NM_001084	No

ORF, open reading frame; ND, not determined.

the RAF family of serine/threonine kinases, and phosphorylates MEK1 [16]. It had not been known whether an overexpression of wild ARAF1 protein has a transforming activity.

3.2. *ARAF1* as an oncogene

We thus determined the whole nucleotide sequence of our *ARAF1* cDNA (cDNA clone ID #7). The sequence is 2441 bp, and contains an open reading frame (spanning nucleotide position 126–1943) encoding a protein of 606 amino acids, which is identical to ARAF1 (Fig. 2(b)). Within the protein-coding region, there is only one nucleotide mutation compared to the published *ARAF1* cDNA sequence; a "T" at nucleotide position 1550 in the reported sequence (NM_001654) is replaced with a "C" in our sequence. The codon sequence "TTG" at the amino acid position 450 of ARAF1 is thus changed to "CTG" in our cDNA. However, both codons encode the same leucine residue, and thus the mutation does not affect the protein sequence.

To confirm that mere overexpression of wild ARAF1 protein has a transforming activity, we repeated the focus formation assay with the retrovirus generated from our *ARAF1* cDNA. As shown in Fig. 2(c), the recombinant virus reproducibly induced transformed foci (30–50 foci per microgram of the input plasmid) in the recipient 3T3 cells. The transforming ability of ARAF1 was also tested by the tumorgenicity assay with athymic nude mice. The 3T3 cells infected with the empty virus or retrovirus expressing ARAF1 or v-Ras were inoculated subcutaneously into nude mice. As shown in Fig. 2(d), tumour formation was observed in all mice for the latter 2 cases, arguing that ARAF1 has oncogenic potential.

3.3. Expression of *ARAF1* in PDC

We finally measured the expression level of *ARAF1* mRNA in PDC by the quantitative real-time reverse

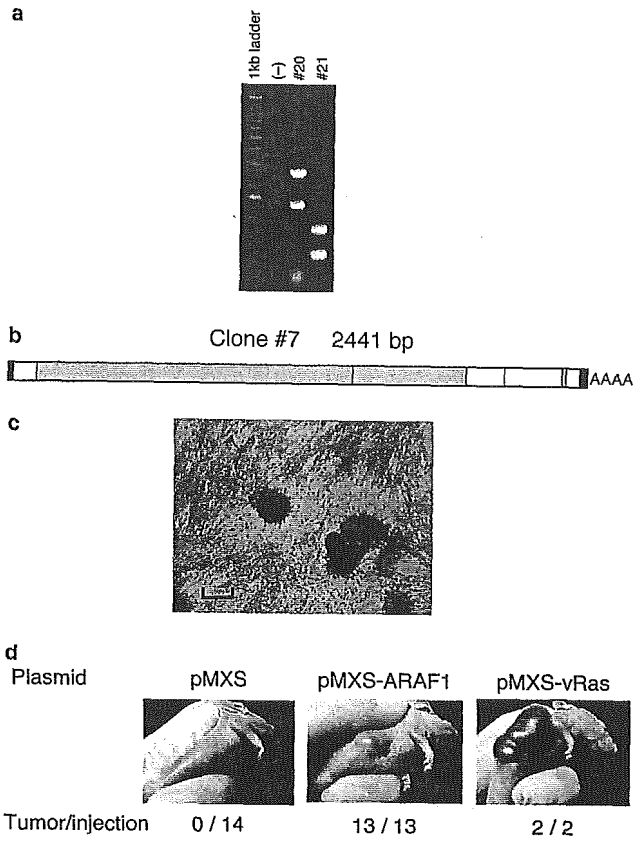

Fig. 2. Identification of the transforming *ARAF1* gene. (a) Genomic DNAs isolated from the transformed foci (cell clone ID #20 and #21) were subjected to PCR. A PCR without DNA template was also conducted as a negative control (−). DNA size markers (1 kb DNA ladder; Invitrogen) are electrophoresed at the left. (b) A 3T3 clone yielded a PCR product of 2441 bp long (cDNA clone ID #7). The cDNA has a protein-coding region (gray) for 606 amino acids that was identical to human ARAF1 protein. Nucleotides that did not match the published *ARAF1* cDNA are indicated by red lines. (c) Our ARAF1 cDNA was ligated to pMXS, and used to generate recombinant virus. Infection with the virus induced multiple transformed foci in 3T3 cells. Scale bar, 100 μm. (d) 3T3 cells (5×10^5) were cultured for two days with retrovirus made from pMXS, pMXS-ARAF1 or pMXS-vRas plasmid, and were injected subcutaneously into nu/nu mice. Tumour formation was examined after 4 weeks.

transcription (RT)-PCR method. As shown in Fig. 3, all 3 PDC cell lines express similar amounts of *ARAF1* mRNA. In addition, we quantified *ARAF1* mRNA in human clinical specimens. Pancreatic juice from patients with PDC contains cancer cells (transformed ductal cells) in addition to normal ductal cells and blood cells. The former two fractions were purified, by an affinity column for MUC1 surface protein [12], from pancreatic juice of PDC patients ($n = 14$). Such purified fractions should be highly enriched for PDC cells [13]. Similar MUC1-positive fractions were also purified from the pancreatic juice of healthy individuals ($n = 7$). Quantification of *ARAF1* mRNA revealed that its mRNA level was highly elevated in six out of the 14 patient, but not in the specimens from healthy individuals. These data

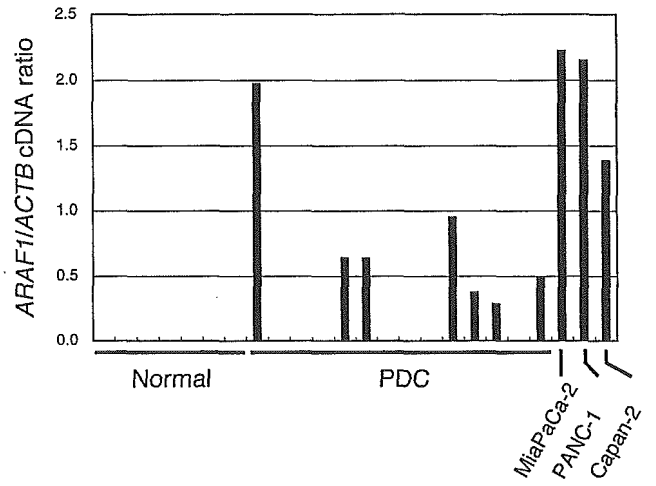

Fig. 3. Quantification of *ARAF1* mRNA. Complementary DNA was prepared from PDC cell lines (MiaPaCa-2, PANC-1 and Capan-2) or $MUC1^+$ ductal cell preparations purified from healthy individuals (Normal) or patients with PDC, and were then subjected to real-time RT-PCR analysis with primers specific for the *ARAF1* or *ACTB* genes. The ratio of the abundance of *ARAF1* mRNA to that of *ACTB* mRNA was calculated as 2^n, where n is the C_T value for *ACTB* cDNA minus the C_T value for *ARAF1* cDNA.

indicate that the transcription of *ARAF1* is selectively activated in PDC cells.

4. Discussion

In this manuscript, we have constructed a retroviral cDNA expression library of PDC. Since 90% (27/30) of the viral plasmids carried cDNA inserts and since the overall clone number was >2 millions, our library should cover nearly all transcriptome in MiaPaCa-2 cells.

RAF family is composed of RAF1, ARAF1 and BRAF in humans. All these serine/threonine kinases are believed to act downstream of RAS-family proteins, and to phosphorylate and regulate downstream MAP kinase kinases (MAPKKs). Many studies have revealed transforming potentials of RAF family proteins. RAF was originally identified as a cellular homologue of viral oncoprotein, v-Raf [17]. Deletion of amino-terminal regions unmasks the transforming ability of RAF1 [18] and ARAF1 [19]. On the other hand, somatic point mutations have been found in the *BRAF* gene among clinical specimens of colorectal carcinoma [20]. Such mutations were shown to induce transforming activity in BRAF protein. In contrast to *BRAF*, somatic point mutations are rarely found in *ARAF1* gene [21].

Overexpression of wild forms of RAF1 or BRAF failed to exert a transforming activity [18,20]. Although deletion/truncation of amino terminal regions of ARAF1 induced transformed foci in 3T3 fibroblasts [22] and abrogated cytokine-dependency in hematopoietic cells [19], it has not been tested whether wild ARAF1 protein has transforming potential. In this manuscript, however, it was unexpectedly revealed that a long terminal repeat-driven expression of ARAF1 induces transformed foci in 3T3 cells, which subsequently generated tumours in immunocompromised mice. Therefore, it has been unveiled here that an overexpression of wild ARAF1 is directly linked with cellular transformation process.

These data also indicate the importance of measuring protein/mRNA amounts of ARAF1 in various human cancers. In this context, it was interesting to find a high expression of *ARAF1* mRNA in fresh clinical specimens of PDC. Our findings shed new light on the understanding of RAF family kinases, and open up the possibility that ARAF is involved in carcinogenesis in human cancers through a previously unexpected mechanism.

Conflict of interest statement

None declared.

Acknowledgments

This work was supported in part by a grant for Third-Term Comprehensive Control Research for Cancer from the Ministry of Health, Labor, and Welfare of Japan; and a grant for "High-Tech Research Center" Project for Private Universities: Matching Fund Subsidy (2002–2006) from the Ministry of Education, Culture, Sports, Science, and Technology of Japan.

References

1. Bornman PC, Beckingham IJ. Pancreatic tumours. *Br Med J* 2001, **322**, 721–723.
2. Rosewicz S, Wiedenmann B. Pancreatic carcinoma. *Lancet* 1997, **349**, 485–489.
3. Goggins M, Kern SE, Offerhaus JA, *et al.* Progress in cancer genetics: lessons from pancreatic cancer. *Ann Oncol* 1999, **10**(Suppl. 4), 4–8.
4. Barton CM, Staddon SL, Hughes CM, *et al.* Abnormalities of the p53 tumour suppressor gene in human pancreatic cancer. *Br J Cancer* 1991, **64**, 1076–1082.
5. Bramhall SR. The use of molecular technology in the differentiation of pancreatic cancer and chronic pancreatitis. *Int J Pancreatol* 1998, **23**, 83–100.
6. Tada M, Omata M, Ohto M. Clinical application of ras gene mutation for diagnosis of pancreatic adenocarcinoma. *Gastroenterology* 1991, **100**, 233–238.
7. Yanagisawa A, Ohtake K, Ohashi K, *et al.* Frequent c-Ki-ras oncogene activation in mucous cell hyperplasias of pancreas suffering from chronic inflammation. *Cancer Res* 1993, **53**, 953–956.
8. Hiyama E, Kodama T, Shinbara K, *et al.* Telomerase activity is detected in pancreatic cancer but not in benign tumours. *Cancer Res* 1997, **57**, 326–331.
9. Uehara H, Nakaizumi A, Tatsuta M, *et al.* Diagnosis of pancreatic cancer by detecting telomerase activity in pancreatic

juice: comparison with K-ras mutations. *Am J Gastroenterol* 1999, **94**, 2513–2518.
10. Aaronson SA. Growth factors and cancer. *Science* 1991, **254**, 1146–1153.
11. Pear WS, Nolan GP, Scott ML, *et al.* Production of high-titer helper-free retroviruses by transient transfection. *Proc Natl Acad Sci USA* 1993, **90**, 8392–8396.
12. Terada T, Ohta T, Sasaki M, *et al.* Expression of MUC apomucins in normal pancreas and pancreatic tumours. *J Pathol* 1996, **180**, 160–165.
13. Yoshida K, Ueno S, Iwao T, *et al.* Screening of genes specifically activated in the pancreatic juice ductal cells from the patients with pancreatic ductal carcinoma. *Cancer Sci* 2003, **94**, 263–270.
14. Onishi M, Kinoshita S, Morikawa Y, *et al.* Applications of retrovirus-mediated expression cloning. *Exp Hematol* 1996, **24**, 324–329.
15. Yoshizuka N, Moriuchi R, Mori T, *et al.* An alternative transcript derived from the trio locus encodes a guanosine nucleotide exchange factor with mouse cell-transforming potential. *J Biol Chem* 2004, **279**, 43998–44004.
16. Wu X, Noh SJ, Zhou G, *et al.* Selective activation of MEK1 but not MEK2 by A-Raf from epidermal growth factor-stimulated Hela cells. *J Biol Chem* 1996, **271**, 3265–3271.
17. Bonner TI, Kerby SB, Sutrave P, *et al.* Structure and biological activity of human homologs of the raf/mil oncogene. *Mol Cell Biol* 1985, **5**, 1400–1407.
18. Ishikawa F, Sakai R, Ochiai M, *et al.* Identification of a transforming activity suppressing sequence in the c-raf oncogene. *Oncogene* 1988, **3**, 653–658.
19. Hoyle PE, Moye PW, Steelman LS, *et al.* Differential abilities of the Raf family of protein kinases to abrogate cytokine dependency and prevent apoptosis in murine hematopoietic cells by a MEK1-dependent mechanism. *Leukemia* 2000, **14**, 642–656.
20. Davies H, Bignell GR, Cox C, *et al.* Mutations of the BRAF gene in human cancer. *Nature* 2002, **417**, 949–954.
21. Lee JW, Soung YH, Kim SY, *et al.* Mutational analysis of the ARAF gene in human cancers. *APMIS* 2005, **113**, 54–57.
22. Beck TW, Huleihel M, Gunnell M, *et al.* The complete coding sequence of the human A-raf-1 oncogene and transforming activity of a human A-raf carrying retrovirus. *Nucleic Acids Res* 1987, **15**, 595–609.

Carcinogenesis vol.26 no.12 pp.2078–2085, 2005
doi:10.1093/carcin/bgi184
Advance Access publication July 20, 2005

Screening for genomic fragments that are methylated specifically in colorectal carcinoma with a methylated *MLH1* promoter

Koji Koinuma[1,2], Ruri Kaneda[1], Minoru Toyota[3], Yoshihiro Yamashita[1], Shuji Takada[1], Young Lim Choi[1], Tomoaki Wada[1], Masaki Okada[2], Fumio Konishi[4], Hideo Nagai[2] and Hiroyuki Mano[1,5,*]

[1]Division of Functional Genomics and [2]Department of Surgery, Jichi Medical School, Tochigi 329-0498, Japan, [3]Department of Molecular Biology, Cancer Research Institute, Sapporo Medical University, Hokkaido 060-8556, Japan, [4]Department of Surgery, Omiya Medical Center of Jichi Medical School, Saitama 330-8503, Japan and [5]CREST, Japan Science and Technology Agency, Saitama 332-0012, Japan

*To whom correspondence should be addressed. Tel: +81 285 58 7449; Fax: +81 285 44 7322;
E-mail: hmano@jichi.ac.jp

A subset of colorectal carcinomas (CRCs) is associated with microsatellite instability (MSI) of the genome. Although extensive methylation of CpG islands within the promoter regions of DNA mismatch repair genes such as *MLH1* is thought to play a central role in tumorigenesis for MSI-positive sporadic CRCs, it has been obscure whether such aberrant epigenetic regulation occurs more widely and affects other cancer-related genes *in vivo*. Here, by using methylated CpG island amplification coupled with representational difference analysis (MCA–RDA), we screened genomic fragments that are selectively methylated in CRCs positive for *MLH1* methylation, resulting in the identification of hundreds of CpG islands containing genomic fragments. Methylation status of such CpG islands was verified for 28 genomic clones in 8 CRC specimens positive for *MLH1* methylation and the corresponding paired normal colon tissue as well as in 8 CRC specimens negative for methylation. Many of the CpG islands were preferentially methylated in the *MLH1* methylation-positive CRC specimens, although methylation of some of them was more widespread. These data provide insights into the complex regulation of the methylation status of CpG islands in CRCs positive for MSI and *MLH1* methylation.

Introduction

Colorectal carcinoma (CRC) is one of the leading causes of cancer death in humans. Evidence indicates the existence of two major types of genomic instability in CRCs: chromosomal instability and microsatellite instability (MSI) (1). Whereas chromosomal instability is associated with an abnormal DNA content (such as aneuploidy), inactivation of the tumor suppressor gene *TP53*, and activation of oncogenes (2), MSI is associated with defects in the DNA mismatch repair (MMR) system that result in frameshift mutations in microsatellite repeats, and thereby affect the structure of genes containing such repeats (3).

Although germ-line mutations of MMR genes have been detected in the genome of individuals with hereditary non-polyposis colorectal cancer (4–6), many sporadic CRCs positive for MSI are associated with epigenetic silencing of non-mutated MMR genes (7,8). MSI-positive CRCs are characterized by specific clinicopathologic features and gene mutations. Such tumors occur with a higher frequency in women than in men, develop in the right side of the colon, and manifest a mucinous or poorly differentiated histopathology. Many of the CpG dinucleotides within the promoter region of the MMR gene *MLH1* are methylated in MSI-positive CRCs (9,10), and the *BRAF* gene frequently contains activating mutations in these cancers (11–13). Some genomic fragments have been found to be methylated specifically in such CRCs (7), and an entity of CRC with a CpG island methylator phenotype (CIMP) has been proposed (14). However, the profiles of genes and genomic fragments that become methylated in CRC specimens positive for *MLH1* methylation have remained uncharacterized.

With the use of methylated CpG island amplification coupled with representational difference analysis (MCA–RDA) (15), we have now performed a global screening of pooled genomic DNA from CRC specimens positive or negative for *MLH1* methylation in order to identify differentially methylated genomic fragments. With this approach, we identified hundreds of CpG islands whose methylation was specific to CRCs with a methylated *MLH1* promoter.

Materials and methods

Tumor specimens and cell lines

Tumor specimens were obtained from patients with sporadic CRC who underwent surgical treatment in Jichi Medical School Hospital. Informed consent was obtained from each patient, and the study was approved by the ethics committee of Jichi Medical School. Normal portion of colon tissue was excised from a region >5 cm distant from the cancerous region in every case. Genomic DNA was extracted with the use of a QIAmp DNA Mini kit (Qiagen, Valencia, CA). The MSI status of each tumor was determined on the basis of analysis of nine microsatellite repeat loci as previously described (8). The methylation status of the *MLH1* promoter was also examined in each sample (11).

Colon carcinoma cell lines (Caco-2, HCT116, SW480) were obtained from American Type Culture Collection (Manassas, VA). Caco2 cells were cultured in Dulbecco's modified Eagle's medium (DMEM)-F12 (Invitrogen, Carlsbad, CA) supplemented with 10% fetal bovine serum (FBS) (Invitrogen) and 2 mM L-glutamine. HCT116 and SW480 cells were maintained in McCoy's 5A medium (Invitrogen) and Leibovitz's L-15 medium (Invitrogen), both supplemented with 10% FBS, respectively.

MCA–RDA

Genomic DNA from four tumor specimens positive for *MLH1* methylation was mixed and used as a 'tester' sample, whereas that from four specimens negative for *MLH1* methylation was used as a 'driver.' MCA–RDA was performed with the two pooled DNA samples as previously described (15). In brief, both the tester and the driver DNA samples (5 μg of each) were digested first with the SmaI endonuclease (New England Biolabs, Beverly, MA) and then with

Abbreviations: CRC, colorectal carcinoma; COBRA, combined bisulfite restriction analysis; CIMP, CpG island methylator phenotype; EGF, epidermal growth factor; GDF, growth-differentiation factor; MSI, microsatellite instability; MMR, mismatch repair; PCR, polymerase chain reaction; TGF-β, transforming growth factor-β.

XmaI (New England Biolabs), and the resulting fragments were ligated to the RMCA adapter (15). Amplification of methylated CpG islands was achieved by polymerase chain reaction (PCR) with the RMCA24 primer. The amplified fragments of the tester-DNA and driver-DNA were digested with XmaI and SmaI, respectively. The tester amplicons were then ligated to the JMCA adapter and subjected to annealing with an excess amount of the driver amplicons. PCR with the JMCA24 primer then amplified only the tester-specific amplicons. Another round of amplification was performed with the NMCA adapter and the NMCA24 primer (15). The final products were digested with XmaI and ligated into XmaI-digested pBlueScript (Stratagene, La Jolla, CA) for nucleotide sequencing.

Combined bisulfite restriction analysis (COBRA)

The methylation status of isolated clones was tested by the COBRA method (16). The genomic DNA was denatured, incubated for 16 h at 55°C in 3.1 M sodium bisulfite, and then subjected to PCR to amplify CpG islands. The PCR products were digested with a restriction endonuclease, and the resulting fragments were fractionated by polyacrylamide gel electrophoresis (PAGE). The gel was stained with SYBR Green I (Takara Bio, Shiga, Japan) and scanned with an LAS3000 imaging system (Fuji Film, Tokyo, Japan). Genomic fragments were determined to be positive for CpG methylation if ≥10% of the PCR products were cleaved by the restriction endonuclease. The PCR primers and endonucleases used for COBRA are shown in the Supplementary Table online.

For bisulfite sequencing of the *BMP3* promoter, genomic DNA isolated from cancer specimens or cell lines was treated with sodium bisulfite (11) and then subjected to PCR with the primers 5′-AGTTAGAGAGYGAAAGAAT-TAAG-3′ and 5′-ATACAACRAAATAACRACCAACC-3′. The PCR product was ligated into pGEMT-easy (Promega, Madison, WI).

Real-time reverse transcription-polymerase chain reaction (RT–PCR)

Total RNA was prepared from tester or driver samples with an RNeasy Mini column (Qiagen), treated with RNase-free DNase (Qiagen), and subjected to reverse transcription with PowerScript reverse transcriptase (BD Biosciences Clontech, San Jose, CA) and an oligo(dT) primer. Portions of the resulting cDNAs were subjected to PCR with a QuantiTect SYBR Green PCR kit (Qiagen). The amplification protocol comprised incubations at 94°C for 15 s, 63°C (64°C for *KIT* cDNA) for 30 s, and 72°C for 60 s. Incorporation of the SYBR Green dye into PCR products was monitored in real time with an ABI PRISM 7900HT sequence detection system (PE Applied Biosystems, Foster City, CA), thereby allowing determination of the threshold cycle (C_T) at which exponential amplification of PCR products begins. The C_T values for DNA molecules corresponding to the β-actin gene (*ACTB*) and to genomic fragments of interest were used to calculate the abundance of the latter relative to that of the former. The oligonucleotide primers for PCR were 5′-CCATCAT-GAAGTGTGACGTGG-3′ and 5′-GTCCGCCTAGAAGCATTTGCG-3′ for *ACTB*, 5′-AAGTCAACTCCTTGGCCATCTGT-3′ and 5′-TGGAAAAGGT-AACCTCCTCTTTGG-3′ for the bone morphogenetic protein 3 gene (*BMP3*), and 5′-TGACGTCTGGTCCTATGGGATTT-3′ and 5′-TACATTTCAGCA-GGTGCGTGTTC-3′ for *KIT*.

Results

MCA–RDA screening

A total of 249 cases with CRC were examined for their MSI status as well as for methylation in the promoter region of *MLH1*. The majority ($n = 213$) of the tumor specimens from these patients were negative for MSI, while the rest ($n = 36$) were MSI-positive. Also, most of them ($n = 226$) were shown to have no methylation within the *MLH1* promoter (unmethylated group), whereas the remainder ($n = 23$) had a methylated promoter (methylated group) (11). Altogether 16 patients were positive for MSI, but did not have a methylated *MLH1* promoter. On the other hand, three patients were negative for MSI despite the presence of the methylated *MLH1* promoter. The characteristics of the patients examined in the present study are summarized in Table I.

To isolate genes that were specifically methylated in the methylated group, we selected specimens from four men of each group: ID nos 2, 17, 20 and 77 (mean age, 70.0 years) from the methylated group, and ID nos 1, 8, 13 and 31 (mean age, 73.0 years) from the unmethylated group. We have excluded female subjects from the initial screening, since an intense methylation of one X chromosome in female cells may have yielded a large number of pseudopositive clones, methylation status of which may not have linked to the clinical classes, but to lyonization.

Table I. Patient characteristics

ID no.	*MLH1* methylation	MSI status	Age (years)	Sex	Dukes grade
2[a]	Yes	MSS	70	Male	A
17[a]	Yes	MSI	65	Male	B
20[a]	Yes	MSI	76	Male	B
77[a]	Yes	MSI	69	Male	A
225	Yes	MSI	83	Female	C
263	Yes	MSI	86	Female	C
280	Yes	MSI	83	Female	C
305	Yes	MSI	74	Male	B
318	Yes	MSI	76	Female	B
336	Yes	MSI	68	Male	B
413	Yes	MSI	69	Female	A
416	Yes	MSI	76	Female	B
1[a]	No	MSS	65	Male	A
8[a]	No	MSS	89	Male	B
13[a]	No	MSS	74	Male	B
31[a]	No	MSS	64	Male	B
238	No	MSS	74	Male	A
249	No	MSS	62	Male	B
255	No	MSS	69	Female	C
278	No	MSS	73	Male	C
295	No	MSS	71	Female	C
298	No	MSS	70	Male	D
307	No	MSS	80	Female	C
308	No	MSS	62	Male	B
481	No	MSS	59	Male	C

[a]Specimens used for MCA–RDA screening. MSS, microsatellite stable.

Equal amounts of genomic DNA isolated from the four selected tumor specimens of each group were mixed and subjected to MCA–RDA analysis, with the pooled DNA of the methylated group as the tester and that of the unmethylated group as the driver. A total of 384 clones were randomly picked up from the resultant MCA–RDA products, and digestion of the purified plasmid DNA with restriction endonucleases revealed that 294 out of the 384 clones carried the insert fragments. Nucleotide sequencing of such 294 clones indicated that 209 of the clones were found to contain CpG islands. Screening of human genome databases (http://www.ncbi.nlm.nih.gov/BLAST/ and http://genome.ucsc.edu/cgi-bin/hgBlat) with these sequences revealed that 186 of them were localized within or in close proximity to characterized or uncharacterized human genes (112 independent genes).

Candidate genes for differential methylation

The GenBank accession numbers and annotation information for the 112 genes identified by MCA–RDA are shown in Table II. Multiple clones were isolated for a single gene in 33 instances, whereas only one MCA–RDA product was obtained for the remaining genes. The genes listed in Table II were thus candidates for genes whose CpG islands are methylated in a manner dependent on *MLH1* methylation.

We then examined the methylation status of the isolated fragments mapped to the promoter regions. First, we tried to amplify individually by PCR all 70 fragments mapped to the promoter regions in Table II, and could successfully amplify 35 fragments from the pooled DNAs used in MCR–RDA.

Table II. Genes identified by MCA–RDA with CRCs positive or negative for *MLH1* methylation

Gene	GenBank accession no.	No. of MCA–RDA clones	Position of MCA–RDA clones	COBRA data
Homo sapiens, solute carrier family 38, member 3	BC042875	11	Promoter	N.D.
Homo sapiens hypothetical protein MGC29643[a]	AK075487	10	Promoter	compatible
Human progesterone receptor	M15716	6	Exon 1	N.D.
Homo sapiens alpha-1 type XV collagen	L25286	6	Promoter	N.D.
Homo sapiens K-Cl co-transporter KCC4	AF105365	5	Promoter	N.D.
Homo sapiens CGI-150 protein	AF151908	5	3′ region	N.D.
Homo sapiens cDNA *FLJ37615*	AK094934	4	3′ region	N.D.
Human mRNA and promoter DNA for progesterone receptor	X51730	3	Promoter	N.D.
Human arachidonate 12-lipoxygenase mRNA	M62982	3	Promoter	not compatible
Homo sapiens clone IMAGE:5173621	BC031660	3	Promoter	N.D.
Homo sapiens Ras and Rab interactor 1	BC014417	3	3′ region	N.D.
Homo sapiens papilin (PAPLN)[a]	BC042057	3	Promoter	compatible
Homo sapiens F-box and leucine-rich repeat protein 7 (FBXL7)[a]	AB020647	3	Promoter	compatible
Homo sapiens fibronectin type 3 and ankyrin repeat domains 1	BC024189	3	Promoter	not compatible
BX444427 *Homo sapiens* ADULT BRAIN *Homo sapiens* cDNA clone	BX444427	3	Promoter	N.D.
UI-H-BW0-aju-d-09-0-UI.s1 NCI_CGAP_Sub6 *Homo sapiens* cDNA clone	AW297872	2	N.D.	N.D.
Human dystrobrevin-delta	U26742	2	Near 5′ end	N.D.
Homo sapiens, clone IMAGE:5728979	BC035731	2	Promoter	compatible
Homo sapiens ras interactor (RIN1)	L36463	2	Promoter	N.D.
Homo sapiens partial mRNA for doublesex-mab-3 (DM) domain	AJ301580	2	Promoter	not compatible
Homo sapiens mRNA; cDNA DKFZp586D0619	AL834130	2	Promoter	N.D.
Homo sapiens mRNA for NTAK[a]	AB005060	2	Promoter	compatible
Homo sapiens mRNA for FLJ00396 protein	AK090474	2	3′ region	N.D.
Homo sapiens mRNA for dihydropyrimidinase related protein-3 (DPYSL3)[a]	D78014	2	Promoter	compatible
Homo sapiens hypothetical protein MGC35308	BC034775	2	Exon 1	N.D.
Homo sapiens hypothetical protein MGC33600	BC035022	2	N.D.	N.D.
Homo sapiens growth differentiation factor 7 (GDF7)[a]	AF522369	2	Promoter	compatible
Homo sapiens gene NXN encoding nucleoredoxin	NM_022463	2	N.D.	N.D.
Homo sapiens clone 24649	AF070591	2	3′ region	N.D.
Homo sapiens cDNA: FLJ21511	AK025164	2	Promoter	not compatible
Homo sapiens solute carrier family 30, member 10 (SLC30A10)[a]	AK090806	2	Promoter	compatible
Homo sapiens beta-parvin	AF237769	2	Promoter	N.D.
603031612F1 NIH_MGC_115 *Homo sapiens* cDNA clone IMAGE:5172891	BI489865	2	Promoter	N.D.
Mus musculus adult male spinal cord cDNA, clone:A330088B02	AK079637	1	N.D.	N.D.
Mus musculus 9.5 days embryo parthenogenote cDNA, clone:B130054P17	AK045275	1	N.D.	N.D.
Mus musculus 12 days embryo spinal ganglion cDNA, clone:D130032D18	AK051302	1	N.D.	N.D.
IL5-EN0086-281100-292-f08 EN0086 *Homo sapiens* cDNA	BF851362	1	N.D.	N.D.
Human receptor tyrosine kinase ligand LERK-7 precursor	U26403	1	Promoter	not compatible
Human solute carrier family 30, member 3 (SLC30A3)[a]	U76010	1	Promoter	compatible
Human platelet-derived growth factor receptor alpha	M21574	1	3′ region	N.D.
Human pephBGT-1 betaine-GABA transporter	U27699	1	3′ region	N.D.
Human oxytocin mRNA	M25650	1	Promoter	N.D.
Human mRNA for KIAA0222 gene	D86975	1	3′ region	N.D.
Human c-kit proto-oncogene (KIT)[a]	X06182	1	Promoter	compatible
Human cell 12-lipoxygenase	M35418	1	Promoter	N.D.
Human bone morphogenetic protein-3 (BMP3)[a]	M22491	1	Promoter	compatible
Human (clone hST3O-1) sialyltransferase	L29555	1	Promoter	N.D.
Homo sapiens, Similar to parathyroid hormone receptor 1	BC031578	1	3′ region	N.D.
Homo sapiens, potassium channel, subfamily K, member 13 (KCNK13)[a]	BC012779	1	Promoter	compatible
Homo sapiens, clone MGC:50339	BC043386	1	N.D.	N.D.
Homo sapiens, clone IMAGE:6041910	BC040712	1	Promoter	N.D.
Homo sapiens, clone IMAGE:5590527	BC040874	1	Promoter	N.D.
Homo sapiens Wilms tumor 1	BC032861	1	Promoter	not compatible
Homo sapiens TRALPUSH[a]	AF399708	1	Promoter	compatible
Homo sapiens Sry-related HMG-box protein	AF270652	1	Exon 1	N.D.
Homo sapiens sialyltransferase 4A, transcript variant 2 (SIAT4A)[a]	BC018357	1	Promoter	compatible
Homo sapiens protein tyrosine phosphatase, receptor type, N polypeptide 2	BC034040	1	3′ region	N.D.
Homo sapiens prostaglandin E2 receptor	L25124	1	Promoter	N.D.
Homo sapiens polyamine modulated factor-1	AF141310	1	3′ region	N.D.
Homo sapiens nuclear receptor subfamily 5, group A, member 1	BC032501	1	3′ region	N.D.
Homo sapiens NEL-like 2 (NELL2)[a]	BC020544	1	Promoter	compatible
Homo sapiens mRNA; cDNA DKFZp667I0324	AL832828	1	N.D.	N.D.
Homo sapiens mRNA; cDNA DKFZp564L0472	AL080101	1	3′ region	N.D.
Homo sapiens mRNA; cDNA DKFZp564G1482	AL136698	1	Promoter	N.D.
Homo sapiens mRNA, chromosome 1 specific transcript KIAA0495	AB007964	1	Promoter	N.D.
Homo sapiens chromosome 13 open reading frame 21 (C13orf21)[a]	BC029067	1	Promoter	compatible
Homo sapiens mRNA for SOX7 protein[a]	AJ409320	1	Promoter	compatible
Homo sapiens mRNA for nephrosis 2, idiopathic, steroid-resistant (NPHS2)[a]	AJ279254	1	Promoter	compatible
Homo sapiens mRNA for MDC2 alpha, MDC2 beta	AB009671	1	Promoter	N.D.
Homo sapiens mRNA for KIAA0641 protein	AB014541	1	N.D.	N.D.

Table II. *Continued*

Gene	GenBank accession no.	No. of MCA–RDA clones	Position of MCA–RDA clones	COBRA data
Homo sapiens mRNA for transcription factor 7-like 1 (TCF7L1)[a]	AB031046	1	Promoter	compatible
Homo sapiens mRNA for calmegin (CLGN)[a]	D86322	1	Promoter	compatible
Homo sapiens mRNA for ADAMTS19 protein[a]	AJ311904	1	Promoter	compatible
Homo sapiens microtubule-associated protein 1B, transcript variant 1	NM_005909	1	Promoter	N.D.
Homo sapiens matrix metalloproteinase-21	AF520613	1	Exon 2	N.D.
Homo sapiens KIAA0534 protein	BC047716	1	Promoter	N.D.
Homo sapiens hypothetical protein MGC49007	BC041175	1	N.D.	N.D.
Homo sapiens hypothetical protein LOC284801	BC036201	1	Promoter	N.D.
Homo sapiens hypothetical protein LOC283887[a]	BC023651	1	Promoter	compatible
Homo sapiens hypothetical protein BC009980	BC009980	1	Promoter	N.D.
Homo sapiens GATA binding protein 2	BC051342	1	Promoter	not compatible
Homo sapiens forkhead-related transcription factor FREAC-9	AF042832	1	Exon 1	N.D.
Homo sapiens erythroblast macrophage protein EMP	AF084928	1	Promoter	N.D.
Homo sapiens Enah/Vasp-like (EVL)[a]	BC023997	1	Promoter	compatible
Homo sapiens cytokine receptor-like factor 1	BC044634	1	Promoter	N.D.
Homo sapiens cystathionine beta-synthase (CBS)[a]	L14577	1	Promoter	compatible
Homo sapiens clone DNA68818 PSST739	AY358393	1	Promoter	N.D.
Homo sapiens ceh-10 homeodomain containing protein	AY336059	1	Exon 1	N.D.
Homo sapiens cDNA FLJ42875	AK124865	1	Promoter	N.D.
Homo sapiens cDNA FLJ41549[a]	AK123543	1	Promoter	compatible
Homo sapiens cDNA FLJ38293	AK095612	1	Promoter	N.D.
Homo sapiens cDNA FLJ37464[a]	AK094783	1	Promoter	compatible
Homo sapiens cDNA FLJ33739	AK091058	1	3′ region	N.D.
Homo sapiens cDNA FLJ14238	AK024300	1	Promoter	N.D.
Homo sapiens cDNA clone IMAGE:6025756	BC064906	1	Promoter	N.D.
Homo sapiens bridging integrator protein-1	U68485	1	3′ region	N.D.
Homo sapiens brain tumor associated protein LRRC4[a]	AF196976	1	Promoter	compatible
Homo sapiens apoptosis-associated tyrosine kinase, mRNA	BC047378	1	3′ region	N.D.
ho64c01.x1 Soares_NFL_T_GBC_S1 *Homo sapiens* cDNA clone	AW873619	1	Promoter	N.D.
Helix pomatia sulfatase 1 precursor	AF109924	1	Promoter	N.D.
H.sapiens mitogen inducible gene mig-2 (MIG2)[a]	Z24725	1	Promoter	compatible
GENCOURT_8532095 NIH_MGC_113 *Homo sapiens* cDNA clone	BU899260	1	N.D.	N.D.
EST379664 MAGE resequences, MAGJ *Homo sapiens* cDNA	AW967589	1	N.D.	N.D.
BX394700 *Homo sapiens* NEUROBLASTOMA COT 25-NORMALIZED	BX394700	1	Promoter	N.D.
AL545903 *Homo sapiens* PLACENTA COT 25-NORMALIZED	AL545903	1	Promoter	N.D.
AGENCOURT_8219616 Lupski_sympathetic_trunk *Homo sapiens* cDNA clone	BQ722471	1	N.D.	N.D.
AGENCOURT_7546470 NIH_MGC_70 *Homo sapiens* cDNA clone	BQ218409	1	Promoter	N.D.
7k34e06.x1 NCI_CGAP_Ov18 *Homo sapiens* cDNA clone IMAGE:3477227	BF058764	1	N.D.	N.D.
602695383F1 NIH_MGC_97 *Homo sapiens* cDNA clone IMAGE:4827284	BG722892	1	N.D.	N.D.
Homo sapiens mRNA for KIAA0711 protein	AB018254	1	3′ region	N.D.
Homo sapiens E2F binding protein	AY152547	1	Exon 1	N.D.
Homo sapiens cDNA FLJ38336	AK095655	1	3′ region	N.D.

N.D., not determined. COBRA data indicated that methylation level of the MCA–RDA clones in CRCs positive for *MLH1* methylation was increased (compatible) or not (not compatible) compared with that in CRCs negative for *MLH1* methylation.
[a]Clones analyzed in a test set of samples.

By using COBRA, their CpG methylation status was assessed among the samples used in MCR–RDA. As indicated in Table II, 28 fragments out of 35 were preferentially methylated in the tester DNA, while 7 of them were not.

The methylation status of such 28 fragments was further tested in clinical specimens that had not been used for the initial screening. This test set included eight cancer specimens positive for *MLH1* methylation and the paired normal colon tissue as well as eight cancer specimens negative for *MLH1* methylation (Table I).

The methylation status of each genomic fragment in the clinical specimens is shown color-coded in Figure 1; fragments with a methylation level of $\geq 10\%$ as determined by COBRA are indicated in red, whereas those with a methylation level of $< 10\%$ are shown in blue. Most genomic fragments were extensively methylated in most or all of the cancer specimens positive for *MLH1* methylation, but not in those negative for *MLH1* methylation. The difference in CpG methylation for the MCA–RDA products between the methylated and unmethylated groups of patients was thus confirmed in a distinct test set of CRC specimens.

A more detailed inspection of the data in Figure 1, however, indicates that the MCA–RDA products can be separated into three subgroups on the basis of their methylation profiles. The genomic fragments in the first group (*MIG2* to *NPHS2* in Figure 1) were also methylated in $\geq 25\%$ of the paired normal colon tissue samples. The fragment corresponding to *MIG2*, for instance, was methylated in all of the *MLH1* methylation-positive cancer specimens and the respective normal tissue. Methylation of these genomic regions thus probably occurred in each patient before the development of CRC and might be related to the aging process.

The genomic fragments in the second group (*BMP3* to *DPYSL3*) were not methylated in normal colon tissue but were methylated in $\geq 25\%$ of cancer specimens that were negative for *MLH1* methylation. The methylation of these

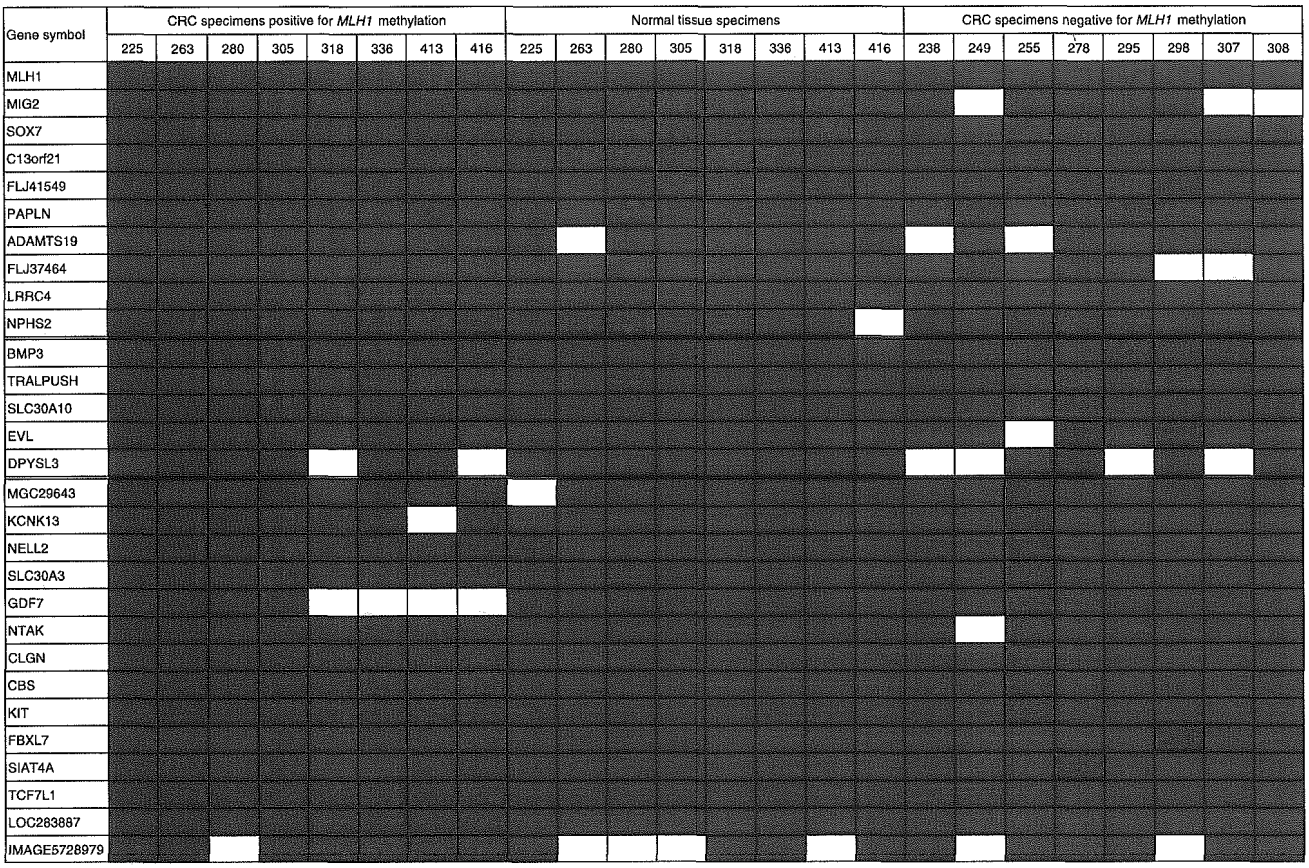

Fig. 1. Gene methylation profiles of CRC specimens. Twenty-eight clones were randomly chosen from the MCA–RDA products of the selected study specimens, and their methylation status (plus that of *MLH1*) was determined by COBRA in CRC specimens positive for the methylation of the *MLH1* promoter ($n = 8$), their paired normal colon tissue samples, and CRC specimens negative for *MLH1* methylation ($n = 8$). Each column represents a clinical specimen (ID numbers are shown), and each row indicates a gene corresponding to an MCA–RDA product. Red box, methylated gene; blue box, unmethylated gene; white box, not examined.

fragments thus appeared to be specific to the cancerous state with a slightly increased prevalence among *MLH1* methylation-positive CRC.

The fragments in the third group (*MGC29643* to *IMAGE5728979*) were methylated in <25% both of normal specimens and of cancer specimens negative for *MLH1* methylation. The methylation of these genes thus appears to be regulated in concert with that of *MLH1*.

Analysis of BMP3

Among the genomic clones analyzed, we first focused on that corresponding to BMP3. BMP3 is a member of the transforming growth factor-β (TGF-β) superfamily of proteins that also includes TGF-β1, TGF-β2, TGF-β3, Mullerian inhibitory substance, BMP2A, BMP2B, BMP6, growth-differentiation factor (GDF) 5, GDF6 and GDF7 (17,18). Members of this protein superfamily exert inhibitory effects on various human cancers through activation of their cognate receptors and SMAD proteins (19,20). BMP2, for instance, induces both the activation of the p38 isoform of mitogen-activated protein kinase and apoptosis in medulloblastoma cells (21). Although little is known of the physiological functions of BMP3, it is possible that this protein also possesses antitumor activity and that its expression is epigenetically regulated in cancer cells. Interestingly, Dai *et al.* (22) have recently reported that *BMP3* promoter is methylated frequently (~50%) in non-small-cell lung carcinoma, which many imply that dysfunction of BMP3 may be commonly involved in the carcinogenesis of a wide range of human tumors.

The COBRA assay revealed that the MCA–RDA clone corresponding to the promoter region of *BMP3* was methylated in CRC specimens that were positive or negative for *MLH1* methylation (Figures 1 and 2A). Further, as shown in Figure 2B, detailed analysis of the methylation status of the *BMP3* promoter by sequencing of DNA fragments after sodium bisulfite treatment revealed extensive hemi- or biallelic methylation of the promoter in CRC specimens positive for *MLH1* methylation (ID nos 225, 318 and 481) but not in one negative for *MLH1* methylation (ID no. 249). CpG methylation throughout the promoter fragment was also evident in CRC cell lines positive (HCT116) or negative (Caco2) for *MLH1* methylation, but not in the *MLH1* methylation-negative line SW480. Together with the COBRA data in Figure 1, these results suggest that the promoter region of *BMP3* is methylated in all clinical specimens and cell lines positive for methylation of the *MLH1* promoter as well as in some specimens and cell lines negative for *MLH1* methylation.

We then examined whether the epigenetic changes in the *BMP3* promoter affected its transcriptional activity. Quantitative real-time RT–PCR analysis revealed that *BMP3*

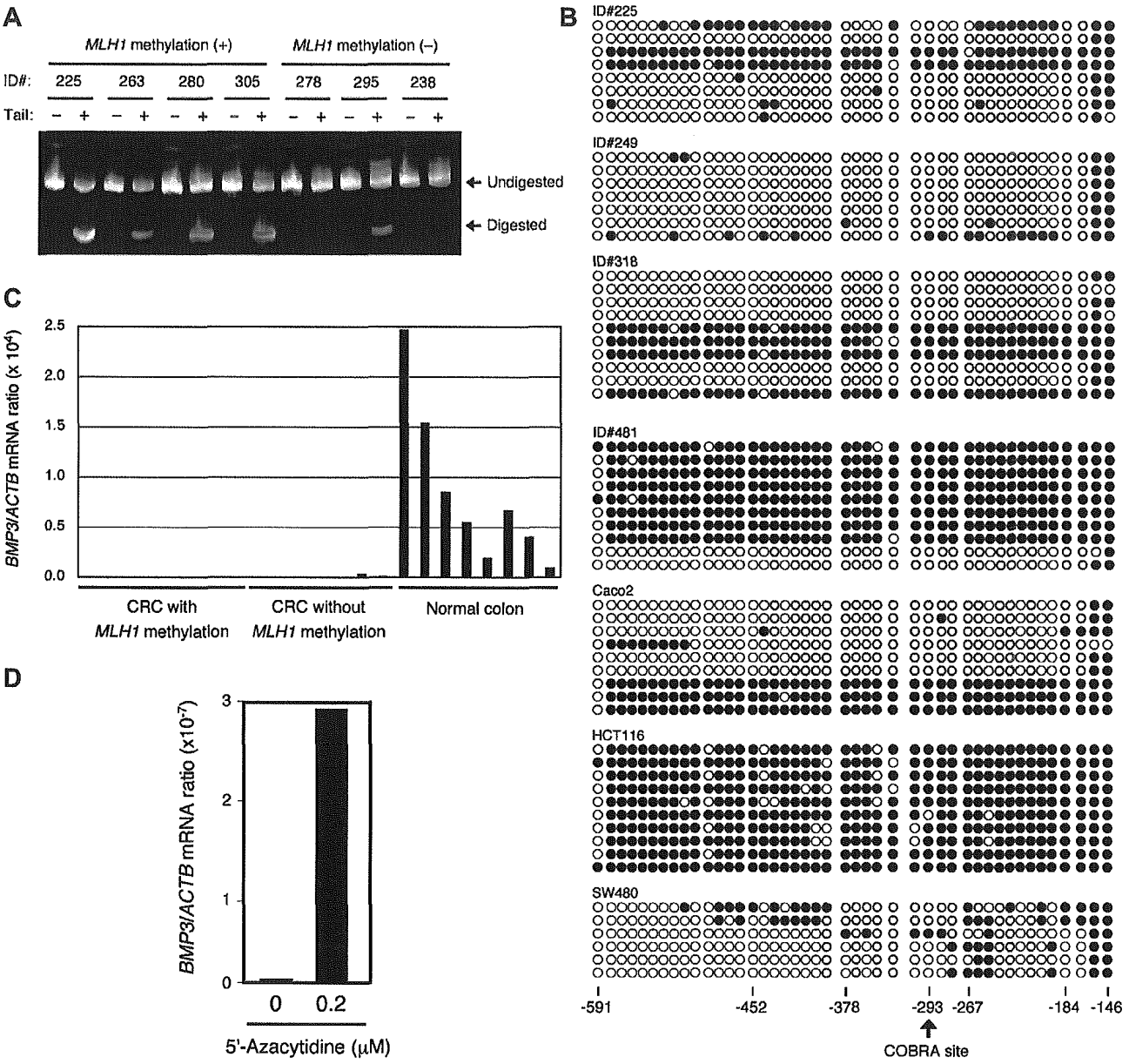

Fig. 2. Methylation status of the *BMP3* promoter and *BMP3* expression in CRC specimens. (**A**) The methylation status of the promoter region of *BMP3* in the indicated clinical specimens was examined by COBRA. Sensitivity of PCR products to digestion with TaiI is indicative of methylation of the CpG island examined. (**B**) Genomic DNA of the indicated clinical specimens and CRC cell lines (Caco2, HCT116 and SW480) was treated with sodium bisulfite, after which the *BMP3* promoter region was amplified by PCR and sequenced. Closed and open circles indicate methylated and unmethylated CpG islands, respectively. The nucleotide positions of the CpG islands (numbered relative to the transcriptional start site) are indicated at the bottom, and the TaiI digestion site for COBRA in (A) is shown by the arrow. (**C**) The level of expression of *BMP3* relative to that of *ACTB* in clinical specimens was determined by quantitative RT–PCR. (**D**) HCT116 cells were incubated for 72 h with or without 0.2 μM of 5′-azacytidine, and were then subjected to RT–PCR analysis for determination of the amount of *BMP3* mRNA relative to that of *ACTB* mRNA.

was transcriptionally silent in CRC specimens positive for *MLH1* methylation (Figure 2C), in which the *BMP3* promoter was also extensively methylated. In contrast, *BMP3* mRNA was abundant in the paired normal colon tissue samples. Although *BMP3* expression was detected in some CRC specimens negative for *MLH1* methylation, the level of expression was greatly reduced compared with that in normal colon tissue. These data thus indicate that *BMP3* transcription is suppressed in most CRCs.

In order to directly examine the relationship between promoter methylation and gene silencing of *BMP3*, HCT116 cells were incubated for 3 days with 5′-azacytidine, an inhibitor of *de novo* methylation of genomic DNA. Interestingly, treatment with 5′-azacytidine markedly induced the amount of *BMP3* mRNA in the cells (Figure 2D) and demethylation of its promoter region as well (data not shown). Therefore, extensive methylation of the *BMP3* promoter region should be directly linked to the suppression of its transcription.

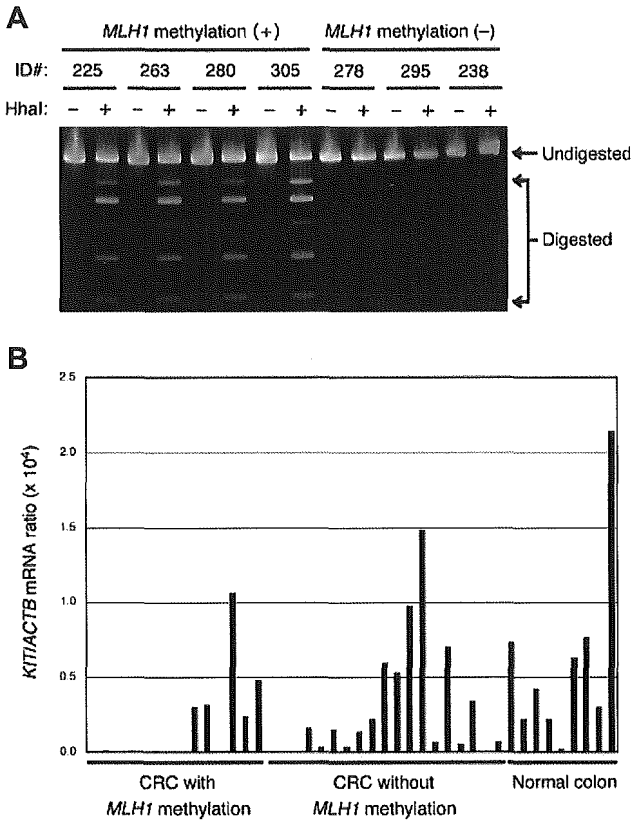

Fig. 3. *Methylation status of the KIT promoter and KIT expression in CRC specimens.* (**A**) The methylation status of the promoter region of *KIT* in the indicated clinical specimens was examined by COBRA. Sensitivity of PCR products to digestion with HhaI is indicative of methylation of the CpG island examined. (**B**) The level of expression of *KIT* relative to that of *ACTB* in clinical specimens was determined by quantitative RT–PCR.

Analysis of KIT

KIT encodes a receptor tyrosine kinase for stem cell factor. Point mutations in *KIT* that increase the kinase activity of the encoded protein have been identified in human gastrointestinal stromal tumors (23), suggestive of a causative role for KIT in these tumors. The expression and activation status of KIT in CRCs have been unclear, however (24,25). We therefore analyzed the methylation status of the *KIT* promoter region in our samples.

Methylation of the *KIT* promoter was highly restricted to CRC specimens positive for *MLH1* methylation (Figures 1 and 3A). However, the abundance of *KIT* mRNA did not necessarily match the methylation status of the *KIT* promoter. Despite extensive methylation of the promoter in one CRC sample (ID no.77), for instance, the amount of *KIT* mRNA was relatively high (*KIT/ACTB* mRNA ratio = 4.78×10^{-5}), indicating that promoter methylation might not be a major determinant of transcriptional activity. It is possible, however, that our COBRA analysis revealed the methylation status of a CpG site that is not important for *KIT* transcription.

The mean expression level of *KIT* in the *MLH1* methylation-positive CRC specimens [*KIT/ACTB* mRNA ratio, $1.72 \times 10^{-5} \pm 3.02 \times 10^{-5}$ (mean ± SD)] was significantly lower than that in normal colon tissue ($6.03 \times 10^{-5} \pm 6.29 \times 10^{-5}$; $P = 0.038$, Student's *t*-test). The level of *KIT* expression in CRCs negative for *MLH1* methylation ($2.92 \times 10^{-5} \pm 1.61 \times 10^{-5}$) was also lower than that in normal colon tissue, but this difference was not significant ($P = 0.123$). It is therefore likely that *KIT* is not overexpressed in CRCs.

Discussion

We have screened for genomic fragments whose CpG islands are selectively methylated in CRC specimens positive for methylation of the *MLH1* promoter region. We could readily identify hundreds of genomic fragments with CpG islands that were expected to be differentially methylated between CRCs with or without *MLH1* methylation. Twenty-eight such clones (Table II) were indeed proved to be preferentially methylated in the four CRC specimens positive for *MLH1* methylation compared with the four samples negative for *MLH1* methylation, both of which were used in the original MCA–RDA screening (data not shown).

To verify the selective methylation of these clones, we performed COBRA with a different set of specimens including eight CRCs with *MLH1* methylation and their paired normal tissue samples as well as eight CRCs without *MLH1* methylation. Although all the 28 clones examined were preferentially methylated in the CRC specimens positive for *MLH1* methylation, their methylation profiles among the specimens were not identical, indicating that all CpG methylation observed in MSI-positive CRCs was not specific to this subtype of tumor.

The methylation of certain genomic fragments (14 out of 28 clones examined), however, was highly specific to CRCs that manifested *MLH1* methylation. Almost 50% of the genes were thus methylated in a parallel manner to the CpG methylation of the *MLH1* gene, indicating that a subset of genes is specifically methylated in a subset of CRCs. Our data thus support the existence of CIMP-positive CRCs (14), while it would be mandatory for the better characterization of CIMP-positive tumors to further collect co-methylated genes and to define precisely the hallmark genes for the identification of CIMP (26). It would be interesting to examine whether such clearly defined CIMP is associated with certain clinical manifestations.

Genes corresponding to the co-methylated genomic fragments in our assay included those whose function relates to cell proliferation or differentiation. The predicted structure of NELL2, for example, contains epidermal growth factor (EGF)-like repeats (27), which are present in diverse proteins involved in regulation of the cell cycle, cell proliferation, and developmental processes. NTAK is a member of the EGF family of proteins and is a ligand and activator of ErbB protein tyrosine kinases (28). In addition, GDF7 is a member of the TGF-β superfamily (18), and *TCF7L1* is highly homologous to TCF1 which is a target gene of the Wnt-β-catenin signaling pathway (29), and which plays an important role in CRC carcinogenesis. Aberrant epigenetic regulation of these genes may thus contribute to the pathogenesis or clinical features of CRCs positive for *MLH1* methylation.

The MCA–RDA method thus proved to be highly effective for the identification of differentially methylated genes among fresh clinical specimens. Given the high fidelity of this approach, it is likely that a large number of genes (or genomic fragments) are methylated in CRCs in concert with methylation of the *MLH1* promoter. Our study provides a basis for further characterization of the molecular pathogenesis of CRCs classified as MSI. Together with the results of other

studies (7,30), it also suggests the possibility of development of a stratification scheme for CRCs based on genome methylation profile.

Supplementary material

Supplementary material can be found at: http://www.carcin.oxfordjournals.org/

Acknowledgements

This study was supported by a Grant-in-Aid for Third-Term Comprehensive Control Research for Cancer from the Ministry of Health, Labor, and Welfare of Japan, and by a grant for 'High-Tech Research Center' Project for Private Universities: Matching Fund Subsidy (2002–2006) from the Ministry of Education, Culture, Sports, Science, and Technology of Japan.

Conflict of Interest Statement: None declared.

References

1. Lengauer,C., Kinzler,K.W. and Vogelstein,B. (1998) Genetic instabilities in human cancers. *Nature*, **396**, 643–649.
2. Kinzler,K.W. and Vogelstein,B. (1996) Lessons from hereditary colorectal cancer. *Cell*, **87**, 159–170.
3. Ionov,Y., Peinado,M.A., Malkhosyan,S., Shibata,D. and Perucho,M. (1993) Ubiquitous somatic mutations in simple repeated sequences reveal a new mechanism for colonic carcinogenesis. *Nature*, **363**, 558–561.
4. Fishel,R., Lescoe,M.K., Rao,M.R., Copeland,N.G., Jenkins,N.A., Garber,J., Kane,M. and Kolodner,R. (1993) The human mutator gene homolog *MSH2* and its association with hereditary non-polyposis colon cancer. *Cell*, **75**, 1027–1038.
5. Bronner,C.E., Baker,S.M., Morrison,P.T. *et al.* (1994) Mutation in the DNA mismatch repair gene homologue *hMLH1* is associated with hereditary non-polyposis colon cancer. *Nature*, **368**, 258–261.
6. Papadopoulos,N., Nicolaides,N.C., Wei,Y.F. *et al.* (1994) Mutation of a mutL homolog in hereditary colon cancer. *Science*, **263**, 1625–1629.
7. Toyota,M., Ahuja,N., Ohe-Toyota,M., Herman,J.G., Baylin,S.B. and Issa,J.P. (1999) CpG island methylator phenotype in colorectal cancer. *Proc. Natl Acad. Sci. USA*, **96**, 8681–8686.
8. Miyakura,Y., Sugano,K., Konishi,F., Ichikawa,A., Maekawa,M., Shitoh,K., Igarashi,S., Kotake,K., Koyama,Y. and Nagai,H. (2001) Extensive methylation of h*MLH1* promoter region predominates in proximal colon cancer with microsatellite instability. *Gastroenterology*, **121**, 1300–1309.
9. Cunningham,J.M., Christensen,E.R., Tester,D.J., Kim,C.Y., Roche,P.C., Burgart,L.J. and Thibodeau,S.N. (1998) Hypermethylation of the h*MLH1* promoter in colon cancer with microsatellite instability. *Cancer Res.*, **58**, 3455–3460.
10. Veigl,M.L., Kasturi,L., Olechnowicz,J. *et al.* (1998) Biallelic inactivation of h*MLH1* by epigenetic gene silencing, a novel mechanism causing human MSI cancers. *Proc. Natl Acad. Sci. USA*, **95**, 8698–8702.
11. Koinuma,K., Shitoh,K., Miyakura,Y. *et al.* (2004) Mutations of BRAF are associated with extensive h*MLH1* promoter methylation in sporadic colorectal carcinomas. *Int. J. Cancer*, **108**, 237–242.
12. Wang,L., Cunningham,J.M., Winters,J.L., Guenther,J.C., French,A.J., Boardman,L.A., Burgart,L.J., McDonnell,S.K., Schaid,D.J. and Thibodeau,S.N. (2003) BRAF mutations in colon cancer are not likely attributable to defective DNA mismatch repair. *Cancer Res.*, **63**, 5209–5212.
13. Oliveira,C., Pinto,M., Duval,A. *et al.* (2003) BRAF mutations characterize colon but not gastric cancer with mismatch repair deficiency. *Oncogene*, **22**, 9192–9196.
14. Issa,J.P. (2004) Opinion: CpG island methylator phenotype in cancer. *Nat. Rev. Cancer*, **4**, 988–993.
15. Toyota,M., Ho,C., Ahuja,N., Jair,K.W., Li,Q., Ohe-Toyota,M., Baylin,S.B. and Issa,J.P. (1999) Identification of differentially methylated sequences in colorectal cancer by methylated CpG island amplification. *Cancer Res.*, **59**, 2307–2312.
16. Xiong,Z. and Laird,P.W. (1997) COBRA: a sensitive and quantitative DNA methylation assay. *Nucleic Acids Res.*, **25**, 2532–2534.
17. Hogan,B.L. (1996) Bone morphogenetic proteins: multifunctional regulators of vertebrate development. *Genes Dev.*, **10**, 1580–1594.
18. Davidson,A.J., Postlethwait,J.H., Yan,Y.L., Beier,D.R., van Doren,C., Foernzler,D., Celeste,A.J., Crosier,K.E. and Crosier,P.S. (1999) Isolation of zebrafish gdf7 and comparative genetic mapping of genes belonging to the growth/differentiation factor 5, 6, 7 subgroup of the TGF-beta superfamily. *Genome Res.*, **9**, 121–129.
19. Miyazono,K., Kusanagi,K. and Inoue,H. (2001) Divergence and convergence of TGF-beta/BMP signaling. *J. Cell. Physiol.*, **187**, 265–276.
20. Bottinger,E.P., Jakubczak,J.L., Haines,D.C., Bagnall,K. and Wakefield,L.M. (1997) Transgenic mice overexpressing a dominant-negative mutant type II transforming growth factor beta receptor show enhanced tumorigenesis in the mammary gland and lung in response to the carcinogen 7,12-dimethylbenz-[a]-anthracene. *Cancer Res.*, **57**, 5564–5570.
21. Hallahan,A.R., Pritchard,J.I., Chandraratna,R.A., Ellenbogen,R.G., Geyer,J.R., Overland,R.P., Strand,A.D., Tapscott,S.J. and Olson,J.M. (2003) BMP-2 mediates retinoid-induced apoptosis in medulloblastoma cells through a paracrine effect. *Nat. Med.*, **9**, 1033–1038.
22. Dai,Z., Popkie,A.P., Zhu,W.G. *et al.* (2004) Bone morphogenetic protein 3B silencing in non-small-cell lung cancer. *Oncogene*, **23**, 3521–3529.
23. Hirota,S., Isozaki,K., Moriyama,Y. *et al.* (1998) Gain-of-function mutations of c-kit in human gastrointestinal stromal tumors. *Science*, **279**, 577–580.
24. Bellone,G., Silvestri,S., Artusio,E., Tibaudi,D., Turletti,A., Geuna,M., Giachino,C., Valente,G., Emanuelli,G. and Rodeck,U. (1997) Growth stimulation of colorectal carcinoma cells via the c-kit receptor is inhibited by TGF-beta 1. *J. Cell. Physiol.*, **172**, 1–11.
25. Sammarco,I., Capurso,G., Coppola,L. *et al.* (2004) Expression of the proto-oncogene c-KIT in normal and tumor tissues from colorectal carcinoma patients. *Int. J. Colorectal Dis.*, **19**, 545–553.
26. Yamashita,K., Dai,T., Dai,Y., Yamamoto,F. and Perucho,M. (2003) Genetics supersedes epigenetics in colon cancer phenotype. *Cancer Cell*, **4**, 121–131.
27. Watanabe,T.K., Katagiri,T., Suzuki,M., Shimizu,F., Fujiwara,T., Kanemoto,N., Nakamura,Y., Hirai,Y., Maekawa,H. and Takahashi,E. (1996) Cloning and characterization of two novel human cDNAs (NELL1 and NELL2) encoding proteins with six EGF-like repeats. *Genomics*, **38**, 273–276.
28. Higashiyama,S., Horikawa,M., Yamada,K. *et al.* (1997) A novel brain-derived member of the epidermal growth factor family that interacts with ErbB3 and ErbB4. *J. Biochem.*, **122**, 675–680.
29. Castrop,J., van Norren,K. and Clevers,H. (1992) A gene family of HMG-box transcription factors with homology to TCF-1. *Nucleic Acids Res.*, **20**, 611.
30. Toyota,M., Ohe-Toyota,M., Ahuja,N. and Issa,J.P. (2000) Distinct genetic profiles in colorectal tumors with or without the CpG island methylator phenotype. *Proc. Natl Acad. Sci. USA*, **97**, 710–715.

Received April 29, 2005; revised July 10, 2005; accepted July 12, 2005

THE JOURNAL OF BIOLOGICAL CHEMISTRY
Vol. 280, No. 13, Issue of April 1, pp. 12621–12629, 2005
Printed in U.S.A.

Signal Transducers and Activators of Transcription 3 Augments the Transcriptional Activity of CCAAT/Enhancer-binding Protein α in Granulocyte Colony-stimulating Factor Signaling Pathway*

Received for publication, July 26, 2004, and in revised form, January 3, 2005
Published, JBC Papers in Press, January 21, 2005, DOI 10.1074/jbc.M408442200

Akihiko Numata‡, Kazuya Shimoda‡§, Kenjiro Kamezaki‡, Takashi Haro‡, Haruko Kakumitsu‡, Koutarou Shide‡, Kouji Kato‡, Toshihiro Miyamoto‡, Yoshihiro Yamashita¶, Yasuo Oshima‖, Hideaki Nakajima, Atsushi Iwama‡‡, Kenichi Aoki‡, Ken Takase‡, Hisashi Gondo‡, Hiroyuki Mano¶, and Mine Harada‡**

*From the ‡Medicine and Biosystemic Science, Kyushu University Graduate School of Medical Sciences, 3-1-1 Maidashi, Higashi-ku, Fukuoka, Fukuoka, 812-8582, the ¶Division of Functional Genomics, Jichi Medical School, 3311-1 Yakushiji, Kawaguchi-gun, Tochigi, 329-0498, the ‖Department of Clinical Pharmacology, Jichi Medical School, 3311-1 Yakushiji, Kawaguchi-gun, Tochigi, 329-0498, the **Department of Hematopoietic Factors, Institute of Medical Science, University of Tokyo, 4-6-1 Shirokanedai, Minato-ku, Tokyo, 108-8639, and the ‡‡Laboratory of Stem Cell Therapy, Center for Experimental Medicine, Institute of Medical Science, University of Tokyo, 4-6-1 Shirokanedai, Minato-ku, Tokyo, 108-8639, Japan*

The Janus kinase (Jak)-Stat pathway plays an essential role in cytokine signaling. Granulocyte colony-stimulating factor (G-CSF) promotes granulopoiesis and granulocytic differentiation, and Stat3 is the principle Stat protein activated by G-CSF. Upon treatment with G-CSF, the interleukin-3-dependent cell line 32D clone 3(32Dcl3) differentiates into neutrophils, and 32Dcl3 cells expressing dominant-negative Stat3 (32Dcl3/DNStat3) proliferate in G-CSF without differentiation. Gene expression profile and quantitative PCR analysis of G-CSF-stimulated cell lines revealed that the expression of *C/EBPα* was up-regulated by the activation of Stat3. In addition, activated Stat3 bound to CCAAT/enhancer-binding protein (C/EBP)α, leading to the enhancement of the transcription activity of C/EBPα. Conditional expression of C/EBPα in 32Dcl3/DNStat3 cells after G-CSF stimulation abolishes the G-CSF-dependent cell proliferation and induces granulocytic differentiation. Although granulocyte-specific genes, such as the G-CSF receptor, lysozyme M, and neutrophil gelatinase-associated lipocalin precursor (*NGAL*) are regulated by Stat3, only NGAL was induced by the restoration of C/EBPα after stimulation with G-CSF in 32Dcl3/DNStat3 cells. These results show that one of the major roles of Stat3 in the G-CSF signaling pathway is to augment the function of C/EBPα, which is essential for myeloid differentiation. Additionally, cooperation of C/EBPα with other Stat3-activated proteins are required for the induction of some G-CSF responsive genes including lysozyme M and the G-CSF receptor.

The proliferation and differentiation of hematopoietic progenitor cells are regulated by cytokines (1). Among these, granulocyte colony-stimulating factor (G-CSF)[1] specifically stimulates cells that are committed to the myeloid lineage (2). The importance of G-CSF to the regulation of granulopoiesis has been confirmed by the observation of severe neutropenia in mice carrying homozygous deletions of their G-CSF or G-CSF receptor genes (3, 4). Cytokines activate several intracellular signaling pathways, and the Janus kinase (Jak) signal transducers and activators of transcription (Stat) pathway is essential for cytokine function (5, 6). The binding of G-CSF to cell surface G-CSF receptors activates Jak1, Jak2, and Tyk2 followed by the activation of Stat1, Stat3, and Stat5 (7–9). Stat3 is the principle protein activated by G-CSF (8, 10). Phosphorylated Stats translocate from the cytoplasm into the nucleus and induce transcription of their target genes within a short period of time. 32Dcl3 cells differentiate to neutrophils following treatment with G-CSF. In contrast to their parental cells, 32Dcl3 cells expressing dominant-negative Stat3 (32Dcl3/DNStat3) proliferate in the presence of G-CSF, but they maintain immature morphologic characteristics without evidence of differentiation (11). Additionally, transgenic mice with a targeted mutation of their G-CSF receptor that abolishes G-CSF-dependent Stat3 activation show severe neutropenia with an accumulation of immature myeloid precursors in their bone marrows (12). To clarify the role of Stat3 in the G-CSF signaling pathway, we wished to identify target genes of Stat3.

We found that the levels of CCAAT/enhancer-binding protein (C/EBP) α mRNA were up-regulated following G-CSF stimulation in 32Dcl3 but were unchanged in 32Dcl3/DNStat3. In addition, the activation of Stat3 augmented the function of C/EBPα, which is the essential transcriptional factor for myeloid differentiation. G-CSF-induced granulocytic differentiation was restored in 32Dcl3/DNStat3 cells by the conditional expression of C/EBPα. These results show that one of the major

* This work was supported by a grant of the Japan Leukemia Research Foundation (2002) and Grants-in-aid for Scientific Research 11307015 and 15390302 from the Ministry of Education, Science, Sports, and Culture in Japan. The costs of publication of this article were defrayed in part by the payment of page charges. This article must therefore be hereby marked "*advertisement*" in accordance with 18 U.S.C. Section 1734 solely to indicate this fact.

§ To whom correspondence should be addressed. Tel.: 81-92-642-5230; Fax: 81-92-642-5247; E-mail: kshimoda@intmed1.med.kyushu-u.ac.jp.

[1] The abbreviations used are: G-CSF, granulocyte colony-stimulating factor; IL, interleukin; C/EBPα, CCAAT/enhancer-binding protein; NGAL, neutrophil gelatinase-associated lipocalin precursor; Jak, Janus kinase; Stat, signal transducers and activators of transcription; DNStat3, dominant-negative Stat3; IRES, internal ribosome entry site; GFP, green fluorescent protein; ER, endoplasmic reticulum; IFN, interferon; PBS, phosphate-buffered saline; GAPDH, glyceraldehyde-3-phosphate dehydrogenase; FACS, fluorescence-activated cell sorter; LUC, luciferase; ERK, extracellular signal-regulated kinase; MAP, mitogen-activated protein; TK, thymidine kinase; 4-HT, 4-hydroxytamoxifen.

roles of Stat3 in the G-CSF signaling pathway is to enhance the function of C/EBPα.

MATERIALS AND METHODS

Cell Culture, Expression Plasmid, and Cytokines—32D clone 3 (32Dcl3) and 32Dcl3/DNStat3 cells (DNStat3 deletes the transactivation domain of Stat3) were cultured in RPMI 1640 supplemented with 10% heat-inactivated fetal bovine serum (ICN, Osaka, Japan), penicillin/streptomycin (Invitrogen), recombinant murine interleukin-3 (IL-3) (Kirin Brewery, Takasaki, Japan), and recombinant human G-CSF (Chugai Pharmaceutical, Tokyo, Japan). 293T cells were cultured in Dulbecco's modified Eagle's medium containing 10% fetal bovine serum, penicillin/streptomycin, and L-glutamine.

For the construction of pTag2A-G-CSF receptor, the human G-CSF receptor cDNA (13) (pHQ3, kindly provided by S. Nagata and R. Fukunaga) was excited from the pBluescipt vector and inserted into the FLAG-tagged mammalian expression plasmid pCMV-Tag2A (Clontech). pcDNA3-rat C/EBPα was described before (14). Stat3 cDNA was amplified by PCR and inserted into pCMV-HA vector (Clontech). Stat3c cDNA was elicited from RCMV-Stat3c (15), kindly given from Dr. Darnell, and inserted into pcDNA3.1 (Clontech). For the construction of pMY-IRES-GFP/C/EBPα-ER, full-length human C/EBPα cDNA was fused in-frame with ligand-binding domain (amino acids 281–599) of mouse estrogen receptor harboring a mutation (G525R) that confers selective responsiveness to 4-hydroxytamoxifen (4-HT). A reporter construct of a minimal TK promoter with CEBP-binding sites (p(C/EBP)2TK) was described previously (14).

Murine recombinant leukemia inhibitory factor, natural IFN-α, and recombinant IFN-γ were purchased from Sigma, HyCult Biotechnology (Uden, The Netherlands), and Peprotech (Rocky Hill, NJ), respectively. For Western blotting, 32Dcl3 cells or 32Dcl3/DNStat3 cells were deprived of IL-3 for 12 h. Then cells were stimulated with G-CSF (10 ng/ml), IL-3 (10 ng/ml), leukemia inhibitory factor (10 ng/ml), IFN-α (1,000 units/ml), or IFN-γ (1,000 units/ml) for 30 min.

Microarray Analysis—32D cl3 and 32Dcl3/DNStat3 cells maintained in IL-3 were washed twice with PBS and starved of cytokine in RPMI 1640 containing 10% fetal bovine serum for 8 h and then stimulated with 10 ng/ml G-CSF. Total RNA was extracted, by the acid guanidinium method, from 32Dcl3 and 32Dcl3/DNStat3 cells before or after the stimulation for 2 h with G-CSF. Double-stranded cDNA synthesized from the total RNA (20 μg/sample) was then used to prepare biotin-labeled cRNA for the hybridization with GeneChip MGU74Avs2 microarrays (Affymetrix, Santa Clara, CA) harboring oligonucleotides corresponding to ~6000 known genes as well as ~6000 expressed sequence tag sequences. Hybridization, washing, and detection of signals on the arrays were performed with the GeneChip system (Affymetrix).

Quantitative Real-time Reverse Transcription-PCR Assay—32Dcl3 and 32Dcl3/DNStat3 cells maintained in IL-3, were washed twice with PBS and starved of cytokines for 8 h and then stimulated with 10 ng/ml G-CSF. Cells were harvested at the indicated times, and total RNA was isolated using Isogen (Nippon gene, Tokyo, Japan) according to the manufacturer's instructions. One microgram of extracted RNA was transcribed in a 20-μl cDNA synthesis reaction using an RNA PCR kit (AMV) (Takara, Tokyo, Japan). Real-time PCR for C/EBPα, G-CSF receptor, lysozyme M, neutrophil gelatinase-associated lipocalin precursor (NGAL), and glyceraldehyde 3-phosphate dehydrogenase (GAPDH) was performed by a TaqMan assay on an ABI 7000 system. PCR primers and probes were designed as follows: murine C/EBPα, sense, 5′-CCA TGT GGT AGG AGA CAG AGA CCT A-3′, and antisense, 5′-CTC TGG GAT GGA TCG ATT GTG-3′; probe FAM-5′-CGG CTG GCG ACA TAC AGT ACA CAC AAG-3′-TAMRA, and sense, 5′-CCA AGA AGT CGG TGG ACA AGA-3′, and antisense, 5′-CGG TCA TTG TCA CTG GTC AAC T-3′; probe FAM-5′-AGC ACC TTC TGT TGC GTC TCC ACG TT-3′-TAMRA; murine G-CSF receptor, sense, 5′-CTA AAC ATC TCC CTC CAT GAC TT-3′, and antisense, 5′-GGC CAT GAG GTA GAC ATG ATA CAA-3′; probe FAM-5′-CAT CTT CTC TGT CCC CAC CGA CCA A-3′-TAMRA; murine lysozyme M, sense, 5′-TGC CTG TGG GAT CAA TTG C-3′, and antisense, 5′-ATG CCA CCC ATG CTC GAA T-3′; probe 5′-FAM-CAG TGA TGT CAT CCT GCA GAC CA-TAMRA-3′; murine NGAL, sense, 5′-GGC CTC AAG GAC GAC AAC A-3′, and antisense, 5′-CAC CAC CCA TTC AGT TGT CAA T-3′; probe 5′-FAM-CAT CTT CTC TGT CCC CAC CGA CCA A-TAMRA-3′, and murine GAPDH sense, 5′-ACG GCA AAT TCA ACG GCA-3′, and antisense, 5′-AGA TGG TGA TGG GCT TCC-3′; probe 5′-FAM-AGG CCG AGA ATG GGA AGC TTG TCA TC-TAMRA-3′. PCR amplifications were performed in a 50-μl volume, containing 4 μl of cDNA template, 50 mM KCl, 10 mM Tris-HCl(pH 8.3), 10 mM EDTA, 60 nM, 200 μM dNTPs, 3 mM $MgCl_2$, 200 nM each primer, 0.625 units of AmpliTaqGold, and 0.25 units of AmpErase uracil *N*-glycosylase. Each amplification reaction also contained 100 nM appropriate detection probe. Each PCR amplification was performed in duplicate, using conditions of 50 °C for 2 min preceding 95 °C for 10 min followed by 40 cycles of amplification (95 °C for 15 s, 60 °C for 1 min). In each reaction, GAPDH was amplified as a housekeeping gene to calculate a standard curve and allow for the correction for variations in target sample quantities. Relative copy numbers were calculated for each sample from the standard curve after normalization to GAPDH by the instrument software.

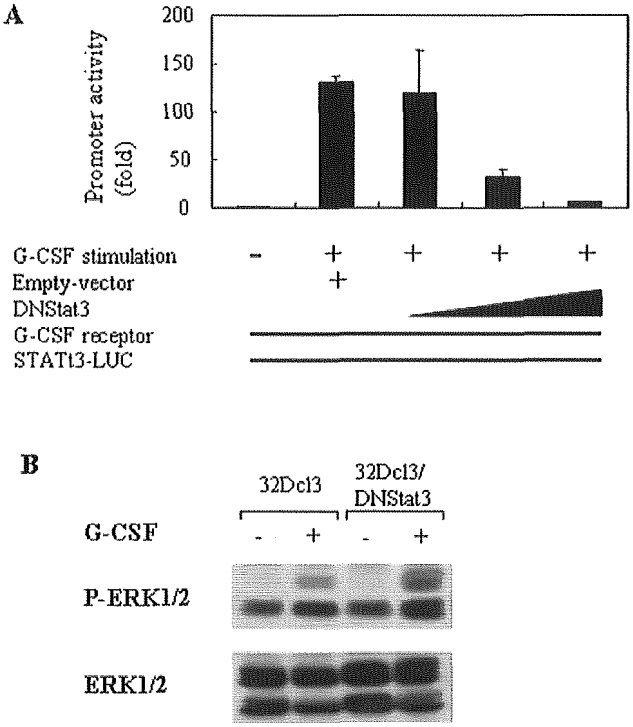

FIG. 1. **The effect of dominant-negative Stat3 on G-CSF signaling pathway.** *A*, transient transfection in 293T cells with a reporter construct with α2-macroglobulin promoter (*STATt3-LUC*), dominant-negative Stat3, and G-CSF receptor. Twelve hours after transfection, cells were stimulated with 10 ng/ml G-CSF. Promoter activity was measured as luciferase activity 36 h after transfection. The *vertical axis number* is the fold induction when compared with control. *B*, 32Dcl3 cells or 32Dcl3/DNStat3 cells were cultured with IL-3 and then deprived of IL-3 for 12 h. Cells were treated with the G-CSF for 30 min and lysed. Post-nuclear supernatants were resolved by 10% SDS-PAGE and transferred to nitrocellulose membranes. Membranes were probed using the indicated antibodies. *p-ERK1/2*, phosphorylated ERK1/2.

Conditional C/EBPα Expression—pMY-IRES-GFP/C/EBPα-ER was transfected into 32Dcl3 and 32Dcl3/DNStat3 cells by electroporation. 5×10^6 cells were transfected with 20 μg of expression vector, and GFP-positive cells were sorted by FACS Vantage (BD Biosciences). Expression of C/EBPα was determined by Western blotting analysis (see below).

Luciferase Assay—293T cells were transfected by the calcium phosphate precipitation method in 6-well plates, and luciferase activity was assayed using a luminometer Lumat LB9507 (Berthold Technologies, Bad Wildbad, Germany) according to the manufacturer's protocol. Each expression plasmid amount was 50–100 ng/well, and the same amount of empty expression vector was used as control, respectively. Results of reporter assays represent the average values for relative luciferase activity generated from five independent experiments.

Flow Cytometry—1×10^7 cells were incubated with 5 μl of recombinant phosphatidylethanolamine-conjugated rabbit anti-murine Gr1 monoclonal antibody (BD Biosciences) for 30 min at 4 °C, washed twice in PBS, and analyzed on a FACS Calibur (BD Biosciences).

Immunoprecipitation and Immunoblotting—Cells were lysed with lysis buffer, and lysates were immunoprecipitated with anti C/EBPβ (Santa Cruz Biotechnology, Santa Cruz, CA) as described previously (8). Total cell lysates or the immunoprecipitates were resolved by 10% SDS-PAGE and transferred to a nitrocellulose membrane. Membranes

TABLE I
Microarray analysis

32Dcl3 and 32Dcl3/DNStat3 cells were starved of cytokines for 8 h and then stimulated or left unstimulated with 10 ng/ml G-CSF. Total RNA was extracted from each fraction and was subjected to the hybridization with high-density oligonucleotide microarrays (MGU74Av2). Fold induction means a rate of increase in gene expression level by G-CSF stimulation. Candidate genes were identified as transcripts that were up-regulated in 32Dcl3 cells and down-regulated or unchanged in 32Dcl3/DNStat3 cells after G-CSF stimulation.

Gene product name	Abbreviation	Accession number	Fold induction	
			32Dcl3	32Dcl3/DNStat3
B-cell leukemia/lymphoma α	Bcl2	L31532	35.6	0.0629
CyclinE1	*Ccne1*	NM007633	29.7	0.690
Serotonin-gated ion channel	*5HT3*	M74425	27.2	0.592
KIF3B protein	*kif3b*	D26077	21.5	0.921
Protein kinase, serine/arginine-specific 1	*Srpk1*	AB012290	18.7	0.321
MAP kinase-interacting serine/threonine kinase 1	*Mknk1*	Y11091	15.7	0.845
Protein tyrosine phosphatase	*Ptpn13*	D83966	12.4	0.964
Transferrin receptor	*Trfr*	X57349	10.6	0.964
Lymphocyte antigen 57	*Ly57*	AF068182	9.62	0.968
Macrophage stimulating 1 receptor	*Mst1r*	X74736	8.83	0.762
Mitogen-activated protein kinase kinase 7	*MKK7*	AB005654	8.14	0.980
RAR-related orphan receptor alpha	*Rorα*	U53228	7.94	0.861
Hemoglobin Y, β-like embryonic chain	*Hbb-y*	V00726	7.38	0.375
Runt related transcription factor 1	*Runx1*	NM009821	7.01	0.226
Microtubule-associated protein 6	*Mtap6*	Y14754	5.06	0.885
CCAAT/enhancer binding protein α	*C/EBPα*	M62362	2.05	0.840
Ecotoropic viral integration site 1	Evi1	M21829	1.55	0.239
Integrin alpha L	*Itgal*	M60778	1.35	0.567
Ninjurin 1	*Ninj1*	U91513	1.34	0.783
Interleukin 17 receptor	*IL17R*	U31993	1.24	0.449
Mucosal addressin	*MAdCAM*	D50434	1.14	0.527
Carbon catabolite repression 4 homolog	*Ccr4*	X16670	1.06	0.0768
Friend leukemia integration 1	*Fli1*	X59421	1.01	0.305

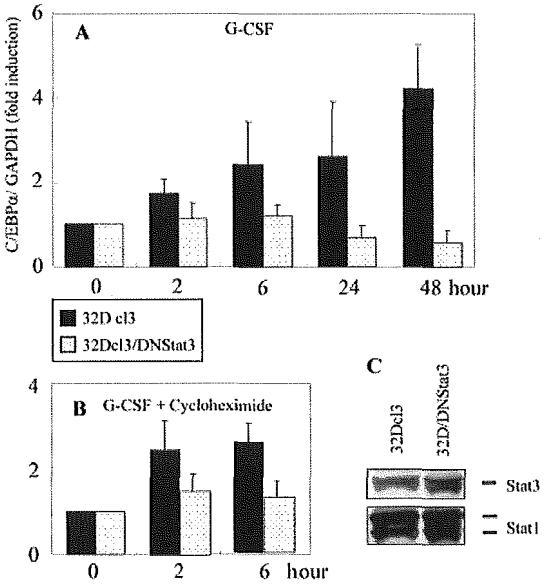

FIG. 2. **Expression of C/EBPα mRNA in G-CSF-stimulated 32Dcl3 and 32Dcl3/DNStat3 cells.** *A* and *B*, 32Dcl3 and 32Dcl3/DNStat3 cells maintained in IL-3 were washed twice with PBS and starved of cytokines for 8 h and stimulated with 10 ng/ml G-CSF (*A*) or 10 ng/ml G-CSF and 10 μg/ml cycloheximide (*B*). Total RNA was isolated from both cell lines at the indicated times and transcribed to cDNA, which was subjected to real-time PCR for murine C/EBPα. The *numbers* given on the *vertical axis* represent the fold induction of the ratios of GAPDH-normalized expression values when compared with those before G-CSF stimulation. Results are expressed as mean fold of two independent experiments.

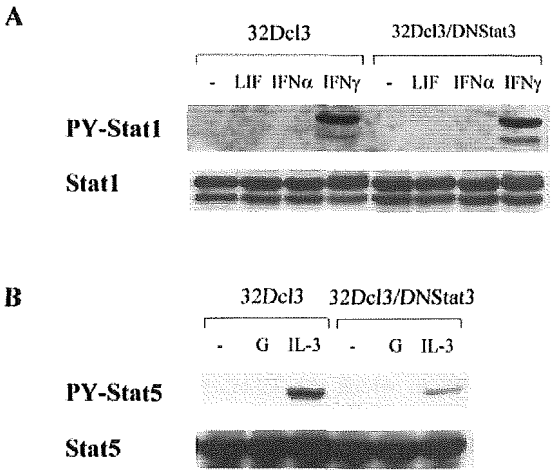

FIG. 3. **The effect of the abrogation of Stat3 on other cytokine signaling pathway.** 32Dcl3 cells or 32Dcl3/DNStat3 cells were cultured with IL-3 and then deprived of IL-3 for 12 h. Cells were treated with the indicated cytokines for 30 min and lysed. Post-nuclear supernatants were resolved by 10% SDS-PAGE and transferred to nitrocellulose membranes. Membranes were probed using the indicated antibodies. *LIF*, leukemia inhibitory factor.

were probed using the indicated antibodies followed by an IgG-horseradish peroxidase-conjugated secondary antibody (Amersham Biosciences) and visualized with the ECL detection system (Amersham Biosciences). Anti-phospho-ERK1/2 antibodies were purchased from Cell Signaling (Beverly, MA). Anti-phospho-Stat1 and -Stat5 antibodies were obtained from New England Biolabs (Beverly, MA), and anti-Stat1, -Stat3, and -C/EBPα antibodies were purchased from Santa Cruz Biotechnology. Membranes were probed using and visualizes with the ECL detection system (Amersham Biosciences).

Proliferation Assay—32D cl3 and 32Dcl3/DNStat3 cells maintained in IL-3 were washed twice with PBS and starved of cytokine for 8 h and then stimulated with 10 ng/ml G-CSF. The number of viable cells was determined by trypan blue dye exclusion using a hemocytometer. [^{3}H[Thymidine incorporation assays were also performed. Briefly, cells (1×10^5) in 100 μl of medium stimulated with murine IL-3 (1.0 ng/ml) or recombinant human G-CSF (10 ng/ml) were cultured for 48 h. During the final 4 h, [^{3}H]thymidine (1μCi/well) was added. Cells were then harvested by filtration, and radioactivity was counted by scintillation spectrophotometer.

RESULTS

G-CSF-induced Intracellular Signal Response in 32Dcl3/DNStat3 Cells—32Dcl3 cells differentiate into neutrophils following treatment with G-CSF, but 32Dcl3 cells expressing a

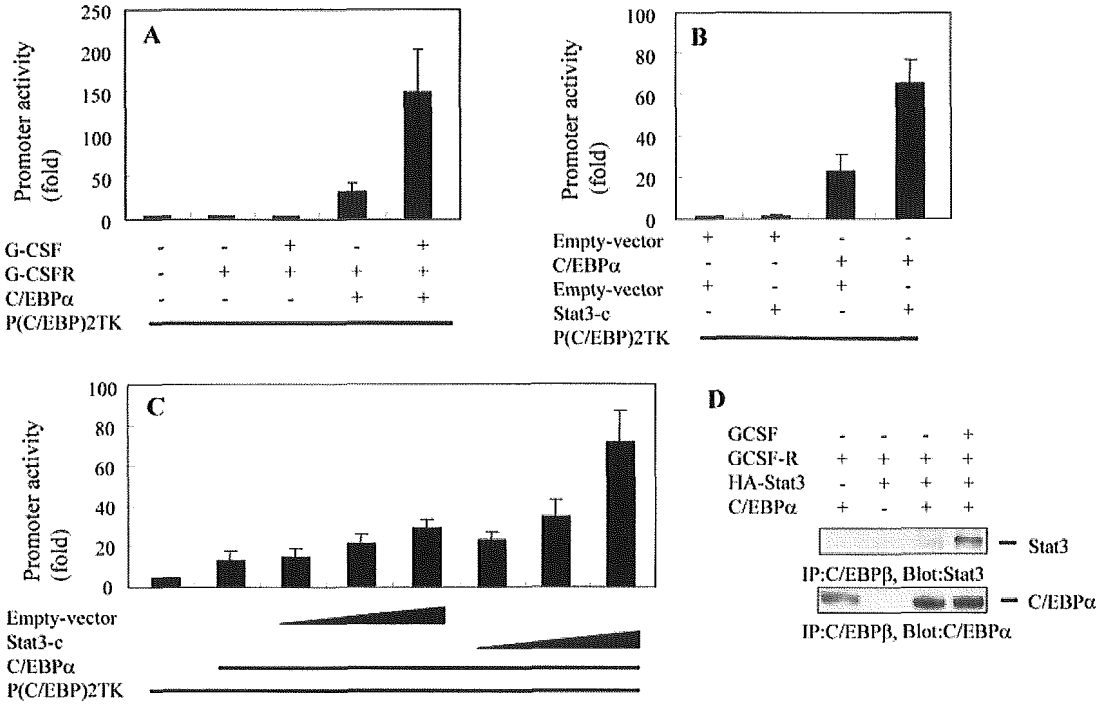

FIG. 4. **Activated Stat3 makes complex with C/EBPα, leading to the enhancement of C/EBPα-induced transcription.** *A*, transient transfection in 293T cells with a reporter construct of a minimal TK promoter with CEBP-binding sites (*p(C/EBP)2TK*), C/EBPα, and G-CSF receptor (*G-CSFR*). Twelve hours after transfection, cells were stimulated with 10 ng/ml G-CSF. Promoter activity was measured as luciferase activity 36 h after transfection. The *vertical axis number* is the fold induction when compared with control. *B* and *C*, transient transfection in 293T cells with a reporter construct of a minimal TK promoter with CEBP-binding sites (*p(C/EBP)2TK*), C/EBPα, Stat3c, and control vectors. Promoter activity was measured as luciferase activity 24 h after transfection. The *vertical axis number* is the fold induction when compared with control. *D*, transient transfection in 293T cells with a construct of G-CSF receptor, HA-Stat3, and C/EBPα and control vectors. After 24 h, cells were lysed and immunoprecipitated (*IP*) with anti C/EBPβ. Cells were stimulated with G-CSF during the final 9 h in the culture. The immunoprecipitates were resolved by 10% SDS-PAGE and transferred to a nitrocellulose membrane. Stat3 was detected by immunoblotting.

dominant-negative Stat3 (32Dcl3/DNStat3) proliferate following G-CSF treatment. These cells maintain immature morphologic characteristics without evidence of differentiation (11). First, we examined the effect of dominant-negative Stat3, carboxyl-truncated Stat3 that lacked 55 amino acids including the transactivation domain. We transfected reporter construct of STATt3-LUC, in which the α2-macroglobulin promoter (16) drives expression of the luciferase (LUC) reporter gene and G-CSF receptor, together with empty vector (pcDNA3) or DNStat3 to 293T cells. After 12 h of transfection, cells were stimulated with 10 ng/ml G-CSF. Cells were cultured for more 24 h, and luciferase assay was performed. As shown in Fig. 1*A*, G-CSF induced the transcriptional activity of Stat3 by 150-fold, and DNStat3 inhibited this G-CSF-induced Stat3 activation in a dose-dependent manner.

G-CSF mainly induces the phosphorylation of Stat3, but it also phosphorylates Stat1 and Stat5 in some cells among the Stats family (8) and induces the activation of MAP kinases. In both 32Dcl3 cells and 32Dcl3/DNStat3 cells, neither Stat1 nor Stat5 was phosphorylated in response to G-CSF (data not shown). As for the MAP kinase activation, the degree of the phosphorylation of ERK1/2 by G-CSF stimulation in 32Dcl3/DNStat3 cells was stronger than that in 32Dcl3 cells (Fig. 1*B*).

Identification of Genes Regulated by Stat3 in the G-CSF Signaling Pathway by Oligonucleotide Array Analysis—To identify Stat3-regulated genes involved in granulocytic differentiation, we compared gene expression change in both cell lines using microarray analysis. 32D cl3 and 32Dcl3/DNStat3 cells maintained in IL-3 were washed twice with PBS and starved in RPMI 1640 containing 10% fetal bovine serum lacking cytokine for 8 h and then stimulated with 10 ng/ml G-CSF. Total RNA was isolated from 32Dcl3 cells and 32Dcl3/DNStat3 cells treated with G-CSF after 0 and 2 h, transcribed to biotin-labeled cRNA, and hybridized to GeneChip MGU74Av2 arrays to compare the expression profile of ~12,000 murine genes. The fold induction in the expression level of each gene was calculated as the ratio of GAPDH-normalized fluorescence intensity value of G-CSF-stimulated cells when compared with those before G-CSF stimulation. As shown in Table I, we could identify a set of candidate genes for Stat3 targets, expression of which was up-regulated in 32D cl3 cells but down-regulated or unchanged in 32Dcl3/DNStat3 cells. Such Stat3-dependent expression profiles were confirmed in triplicate experiments.

C/EBPα Is a Target Gene for Stat3 in G-CSF Signaling Pathway—Among the identified genes, it was decided to focus further efforts on *C/EBPα*. C/EBPα has been shown to be critical for early granulocytic differentiation (17–19), and the factors regulating its activity are unclear. The expression of C/EBPα was examined by real-time quantitative reverse transcription-PCR. C/EBPα mRNA levels are rapidly up-regulated in 32Dcl3 cells, being elevated 2.39-fold after 6 h and 4.20-fold after 48 h (Fig. 2*A*). In contrast to 32Dcl3 cells, the C/EBPα mRNA levels were not changed in 32Dcl3/DNStat3 cells after G-CSF stimulation (Fig. 2*A*). A similar expression pattern was seen in separate experiments with independently designed primers and probes (data not shown). Levels of C/EBPα mRNA were unaffected by cycloheximide treatment (Fig. 2*B*). The expression level of the sum of Stat3 plus dominant-negative Stat3 in 32Dcl3/DNStat3 cells is a little larger than that of Stat3 in 32Dcl3 cells (Fig. 2*C*).

Activated Stat3 Binds to C/EBPα and Enhances the Transcription Activity of C/EBPα—We next examined the effect of

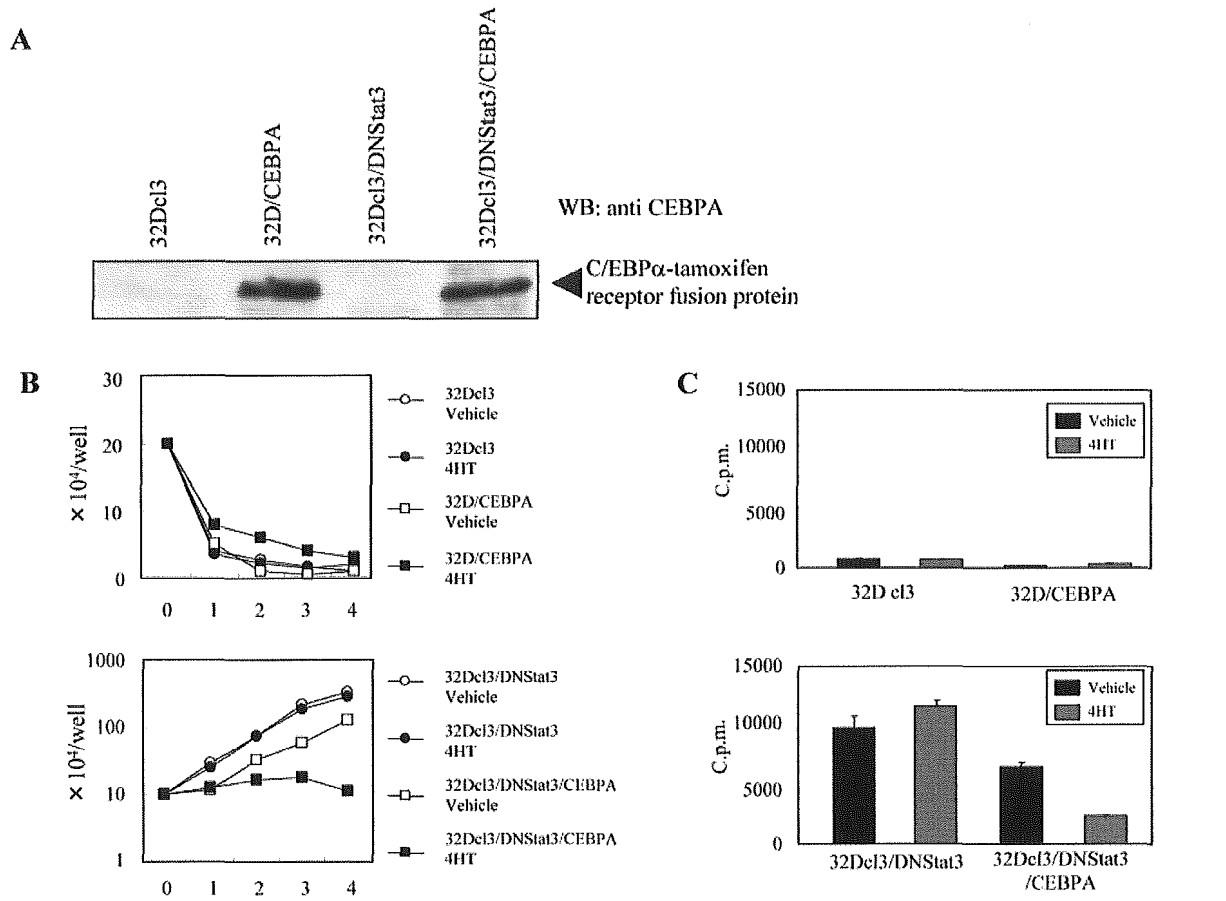

FIG. 5. **Proliferation of 32Dcl3 and 32Dcl3/DNStat3 by restoration of C/EBPα.** *A*, the expression vector pMY-IRES-GFP/C/EBPα-ER was transfected into 32Dcl3 and 32Dcl3/DNStat3 cells. The expression of C/EBPα-ER was examined by Western blotting (*WB*) using anti-C/EBPα polyclonal antiserum. *Lane 1*, 32Dcl3; *lane 2*, 32D/CEBPA; *lane 3*, 32Dcl3/DNStat3; *lane 4*, 32Dcl3/DNStat3/CEBPA. *B*, growth curve of 32Dcl3, 32Dcl3/CEBPA cells (*upper panel*), and 32Dcl3/DNStat3, 32Dcl3/DNStat3/CEBPA cells (*lower panel*). Cells maintained in IL-3 were washed twice with PBS and starved of cytokines for 8 h and stimulated with 10 ng/ml G-CSF plus 0.5 μM 4-HT or vehicle. Viable cells were counted daily by trypan blue dye exclusion method at the indicated times. The *numbers* given on the *vertical axis* represent the mean cell counts (×10⁴/well) of triplicate wells. Standard deviations (S.D.) were less than 15% of each mean. Three independent experiments were performed, and similar results were obtained. Data shown are representative of these results. *C*, ^{3}H incorporation assays in 32Dcl3, 32Dcl3/CEBPA (*upper panel*) and 32Dcl3/DNStat3 and 32Dcl3/DNStat3/CEBPA cells (*lower panel*). Cells maintained in IL-3 were washed twice with PBS and starved of cytokines for 8 h and stimulated with 10 ng/ml G-CSF plus 0.5 μM 4-HT or vehicle for 48 h. During the final 4 h, 1 μCi of [^{3}H]thymidine was added, cells were harvested by filtration, and radioactivity was counted by scintillation spectrophotometer. Results are expressed as mean cpm of triplicate wells ± S.D. Three independent experiments were performed, and similar results were obtained. Data shown are representative of these results.

Stat3 abrogation on the balance of intracellular signals in other cytokine pathways. Although Stat1 was not phosphorylated by leukemia inhibitory factor stimulation in neither 32Dcl3 cells nor 32Dcl3/DNStat3 cells, its activation in response to IFN-γ occurred at the same degree in both 32cl3 cells and 32Dcl3/DNStat3 cells (Fig. 3*A*). As for the Stat5 activation, the phosphorylation of Stat5 by IL-3 stimulation in 32Dcl3 cells was stronger than that in 32Dcl3/DNStat3 cells (Fig. 3*B*). These data indicated that there was the possibility that abrogation of Stat3 signaling can alter the balance of intracellular signals in other cytokine signaling pathways. The transcription of C/EBPα is regulated by C/EBPα itself (20, 21). Then we examined whether activated Stat3 in G-CSF signaling enhance C/EBPα activity or not.

We transfected a reporter construct of a minimal TK promoter with CEBP-binding sites (p(C/EBP)2TK), C/EBPα, and G-CSF receptor to 293T cells. After 12 h of transfection, cells were stimulated with 10 ng/ml G-CSF. Cells were cultured for more 24 h, and a luciferase assay was performed. C/EBPα up-regulated the C/EBPα-dependent gene expression, and the G-CSF stimulation enhanced this C/EBPα-dependent gene expression (Fig. 4*A*). Next we examined the effect of constitutive active Stat3 (Stat3C) on the augmentation of C/EBPα transcriptional activity instead of the G-CSF stimulation. We transfected reporter construct p(C/EBP)2TK, C/EBPα, and Stat3C to 293T cells. After 24 h of transfection, luciferase assay was performed. Stat3C augmented the C/EBPα-dependent gene expression, although Stat3C alone had no influence on the luciferase activity (Fig. 4, *B* and *C*).

As p(C/EBP)2TK contains only a C/EBPα-binding site and does not contain a Stat3-binding sequence, the possibility that Stat3C makes a complex with C/EBPα and augments the function of C/EBPα is raised. Then we transfected C/EBPα, Stat3, and G-CSF receptor to 293T cells and stimulated cells with G-CSF for 6 h. There is no detectable level of endogenous C/EBPα or C/EBPβ protein in 293T cells. Cells were lysed and immunoprecipitated with C/EBPβ antibody (this antibody cross-reacts with C/EBPα). As shown in Fig. 4*D*, immunoprecipitants with anti-C/EBPβ contain Stat3. In addition, the complex formation between C/EBPα and Stat3 is augmented by G-CSF stimulation, indicating that activated Stat3 makes the complex with C/EBPα.

C/EBPα Restores G-CSF-induced Granulocytic Differentiation in 32Dcl3/DNStat3 Cells—To analyze the role of Stat3-